Replies to reviewer 1

> However, it therefore encounters the main difficulties and
> limitations commonly associated with such papers in that
> (i) they often provide only overview statements of the
> (many) methods, with limited justification in some areas,
> to ensure that the paper does not become too long and
> unwieldy; (ii) process representations are inevitably a
> snapshot of understanding at a given time, and therefore
> can lag behind the latest developments in fast moving
> subject areas; and (iii) they generally present few or no
> results to illustrate the performance of the methods and
> tools, these being deferred to future publications where
> they can be presented and discussed in greater detail.
> These inevitable limitations therefore provide some
> difficulties for reviewers when judging a paper of this
> type against some of the GMD review criteria. Although a
> lot of useful information is presented, this paper suffers
> from some limitations in all the identified areas, as
> highlighted in the comments below.
> The authors should therefore consider whether they can
> provide more information and justification on some topics.

We agree that these limitations exist to some extent and have tried to follow the reviewer's specific suggestions as listed below.

> Similarly, some illustration of the impacts of the updates
> (where relevant) might be useful. In practice, the
> simultaneous (or at least imminent) publication of an
> application paper might have been helpful. Several
> (presumably) ongoing and proposed activities are listed in
> Sect. 6, but there are no references to papers by the
> developers that are in press or in preparation.

As requested, we have added more information in the outlook section, showing the principal investigators of the work in progress and manuscripts in preparation.

> Page 2, line 3: MESSy (Modular Earth Submodel System)
> should be defined.

Done.

> Page 2, line 6: Non-methane hydrocarbon (NMHC) chemistry
> is listed as treated, but the term VOC is used everywhere
> else.

We have now added the definition VOCs = CH4 + NMHCs to the text.

> Page 2, line 25: "The rate of 1,4-H-shift for the MACRO2
> radical is treated as predicted by Taraborrelli et al.
> (2012), which is about an order of magnitude lower than
> proposed by Crounse et al. (2012)." However, the Crounse
> et al. (2012) study includes an experimental determination
> and is not simply "proposed" based on theory. Do the
> uncertainties in the theoretical value of Taraborrelli et
> al. (2012) encompass the experimental value of Crounse et
> al. (2012)? If so, surely the Crounse value should be
> applied. If not, further justification for the use of the
> Taraborrelli value is required. In addition to this, I
> could not find any information on this specific reaction
> in Taraborrelli et al. (2012). Is that reference correct?
> It seems that Taraborrelli et al. (2012) considers 1,5
> H-shifts involving transfer of a hydroxyl H atom and 1,6 H
> shifts involving transfer from CH2OH groups (focused on
> OH-isoprene-O2 radicals), whereas Crounse et al. (2012)
> considers the 1,4 H-shift involving transfer of the formyl
> H atom in MACRO2. Are the rates of two different types of
> H-shift reaction therefore being compared?

We thank the referees for spotting this issue and we apologize for it. Taraborrelli et al. (2012) did not consider 1,4-H shifts but after publication, very high-level quantum calculations of corresponding transition state were performed by L. Vereecken (personal communication with DT, 2013).

They resulted in a predicted energy barrier of 20.39 kcal/mol in contrast to the 19.0 kcal/mol reported by Crounse et al. (2012). We actually use the rate expression by Crounse et al. (2012) with an activation energy 1.39 kcal/mol higher. This results in a first-order decomposition rate constant of 0.04 s^{-1}, still much larger than usual atmospheric RO_2 sinks. We have now decided to adopt the rate constant by Crounse et al. (2012). Accordingly, we have modified the sentence

"The rate of 1,4-H-shift for the MACRO2 radical is treated as predicted by Taraborrelli et al. (2012), which is about an order of magnitude lower than proposed by Crounse et al. (2012)."

to

"The rate of the 1,4-H-shift for the MACRO2 radical is now calculated using the expression reported by Crounse et al. (2012)."

> Page 4, section 2.1.1. This section presents a description
> of how the treatment of reactions of OH with VOCs (and
> their degradation products) has been updated, e.g. the use

> of the Peeters et al. (2007) approach for the reactions
> with alkenes. Some additional clarification of the methods
> would be helpful

We have added a table (Table 1) showing the details on the origin of the rate constants and substituents factors that are used.

> i) Although a very useful reference data set, the Atkinson
> et al. (2006) IUPAC evaluation is now quite old. Updates,
> refinements and expansions to the IUPAC evaluation are
> available at http://iupac.pole-ether.fr/. Although some of
> the preferred values may be unchanged from Atkinson et al.
> (2006), it seems strange not to take advantage of the more
> recent information.

Although we neglected to mention this in the manuscript, we actually do consider the IUPAC udates published at http://iupac.pole-ether.fr. This information has now been added to the revised manuscript. References for individual reactions can be found in the file meccanism.pdf in the supplement.

> ii) For the updates to the Kwok and Atkinson SAR method,
> what set of preferred data is being used? Kwok and
> Atkinson used a much larger dataset than covered by
> Atkinson et al. (2006), which (with some exceptions) has a
> cut-off at C3.

Please see the new Table 1 for details.

> iii) On page 4, line 9, it is stated that the substituent
> factors are "... updated or calculated ex novo by
> computing the relative rate coefficient of OH with the
> simplest VOC bearing the substituent relative to the one
> of its parent compound." First of all, it is not clear why
> the substituent factors are based on such a restricted
> dataset. Secondly, it is not at all clear what this means.
> The immediate suggestion is the substituent factor for an
> -OH group (for example) is determined from a comparison of
> the relative rate coefficient for CH3OH and CH4 (which is
> about 140 at 298 K). However, this is not compatible with
> the description of the method further down, which suggests
> the factor is probably actually determined from the rate
> coefficient for CH3OH, in conjunction with the Kwok and
> Atkinson value of kp (and kabst(-OH)). This latter
> procedure would give an F(-OH) value of 5.6 at 298 K,
> which is substantially greater than the Kwok and Atkinson

> value of 3.5, based on optimization to the full dataset of
> OH-containing compounds. If this is the revised method, I
> cannot see that this is any improvement on Kwok and
> Atkinson, and is almost certainly a retrograde step. Given
> that the current MCM uses the Kwok and Atkinson method,
> this would also not support the statement on page 4, line
> 11, "No rigorous evaluation of the SAR has been conducted
> and the estimation uncertainty is expected to be in the
> same range as for the SAR used by the MCM", which surely
> needs some further justification.

We hope that the new Table 1 answers most of these questions. With respect to the quoted sentence, we acknowledge the inaccurate expression mentioning the parent compound. Neither Atkinson (1987) nor Kwok and Atkinson (1995) derived $F(-OH)$ as above but also did not detail how the values 3.4 and 3.5, respectively, were derived. In the last column of our new Table 1, we show how the substituent factor was calculated if it was not adopted from Kwok and Atkinson (1995). Our calculation results in $F^{sec}(-OH) = 3.44$ which is similar to the value from Kwok and Atkinson (1995).

> iv) There are a few other mentions of how the method
> adopts, or differs from, that used with the MCM. On page
> 4, lines 6 and 7 it states that "For the C6 to C11
> species, the MCM rate coefficients are retained." and that
> they "...have no temperature dependence and are only given
> at 298 K." However, inspection of the MCM website
> (http://mcm.leeds.ac.uk/MCM/) reveals that many OH rate
> coefficients for C6-C11 species are temperature dependent
> (e.g. those for C6-C10 n-alkanes). Does the given
> statement therefore mean that MOM is using temperature
> independent rate coefficients derived from the
> temperature-dependent expressions used in the MCM? If so,
> this should be made clearer. It should also be noted that
> the MCM and GECKO-A teams recently published a
> comprehensive update to the way OH rate coefficients are
> to be calculated in the future (Jenkin et al., ACP, 2018),
> although it is recognised that this might be too recent
> for uptake into MOM, and is not yet used in MCM.

We apologize for the confusion. The MCM rate constants for the closed-shell C_6 to C_{11} species are retained. They are mostly constant values (SAR-estimated) but when experimental data is available, a temperature dependence is adopted, e.g. for the toluene + OH reaction. We have corrected the manuscript accordingly replacing

"For the C_6 to C_{11} species, the MCM rate coefficients are retained. It is worth noting that the latter have no temperature-dependence and are only given at 298 K."

with

"For the C_6 to C_{11} closed-shell species, the MCM rate coefficients are retained. It is worth noting that the SAR-estimated ones have no temperature-dependence and are only given at 298 K."

> Page 5, line 1: should CH3CH2O2 be CH3CH2ONO2?

We thank the reviewer for spotting this typo. We have changed the text accordingly.

> Page 8, line 8: Figure 3 is introduced here. Although this
> illustrates the comparative performance of the three
> mechanisms for the given scenario, no further discussion
> of the differences is given.

We have added more information about the model runs presented in Fig. 3. See also our replies to reviewer 2 regarding Fig. 3.

> Is the trace for CB05BASCOE obscured in the
> terpene panel, or are terpenes not represented?

The red line for the terpenes is indeed difficult to see in Fig. 3, it is mostly hidden by the green line. Both MOZART and CB05BASCOE contain similar chemical reactions for lumped terpenes, therefore the results are almost identical.

> Page 10, line 25: The term "Targets" is defined within the
> description of the skeletal reduction method. However,
> elsewhere they seem to be referred to as either "targets"
> or "target species".

Sorry for the confusion. "Targets" and "target species" are synonyms. For consistency, we now only use the term "targets" in the revised text.

Replies to reviewer 2

> Although this type of is important and extremely useful to
> the community as a reference and "one stop shop" for this
> version of the CAABA-MECCA model, I found the paper reads
> very much like a report, listing the work done, and is
> therefore very dry to read. The descriptions of the work
> are basic and not particularly informative as to what has
> been done and why, and the impact of the changes. At the
> moment, the paper is only really useful to an experienced
> user of the CABBA/MECCA modelling tool kit.

We are surprised that the reviewer finds the paper only useful for experienced users. The supplement contains the complete CAABA/MECCA model code as well as a very detailed User Manual. Every reader who is interested in it, can execute the model on their own computer. If there is anything else we can do to improve the accessibility and reproducibility of CAABA/MECCA, we're open for specific suggestions.

> It would have been good to see some impact of the updates
> carried out in terms of an evaluation of the chemical
> mechanistic updates against previous versions of MECCA/MOM
> as well as some evaluation against other chemical
> mechanisms, such as the more detailed benchmark MCM, over
> a range of atmospherically important chemical conditions.
> I realise that this is listed (and it is just a bullet
> pointed list) in the "Summary and outlook" section of the
> paper, but it is not clear if this work has been carried
> out, or is just a goal at the moment. In any case, some
> evaluation of the changes implemented in this version of
> CABBA/MECCA should be included in this paper before it is
> published in GMD.

To illustrate the changes in our model due to the updated MOM chemistry in MECCA, we have now performed 2 additional model runs, one using the simple MIM1 mechanism (Jöckel et al., 2016), and one using the MCM mechanism for isoprene and terpenes. The results have been added to Fig. 3 and to the text of the manuscript. Additional studies which analyze recent versions of MOM under a range of atmospherically important chemical conditions have been presented by Lelieveld et al. (2016), Cabrera-Perez et al. (2016), and Mallik et al. (2018).

> Perhaps mention "community model" in the title?
> (multi-purpose community atmospheric chemistry box
> model..)

We have added "community model" to the title.

> Introduction: A short descriptive definition of
> CABBA/MECCA and its history would be useful

We have added a description of CABBA/MECCA to the introduction.

> 2.1 Mainz Organic Mechanism (MOM) as the title

The title has been changed as requested.

> Page 2, Line 14 "explicit with a low degree of lumping"
> There for the scheme is not explicit!!

We never claimed that the *entire* scheme is explicit. We say that *most* of the oxidation scheme is explicit. Unfortunately, the referee cites only part of our sentence here.

```
> More explanation needed here with respect to "lumping".
```

We added the following text:

Lumping is used for some isomers with similar properties, e.g., the MOM species "LXYL" presents the sum of ortho-, meta- and para-xylene. All lumped species are marked by the prefix "L" in their names.

```
> Page 2, Line 16  The latest version of the MCM is v3.3.1,
> which is focused around a detailed update/evaluation to
> the MCM isoprene chemistry (Jenkin et al., Atmos. Chem.
> Phys., 15, 1143311459, 2015). MIM2 is based on MCMv3.1.
> Therefore, it would be useful to see how the updated MECCA
> model chemistry compares to MCMv3.3.1 in terms of isoprene
> chemistry under a range of representative conditions.
```

As already mentioned above, we have performed an additional model run, using the chemical mechanism of the current MCM for isoprene and terpenes. The results have been added to Fig. 3.

```
> Page 2, Line 25 - Given the last comment, what is the
> justification of not using the experimentally derived
> Crouse et al., (2012) 1,4H-shift kinetic data?
```

This issue has also been raised by referee 1. Please see our reply above.

```
> Page 2, Line 31  Updated aromatic chemistry. Has any
> evaluation of this updated chemistry been carried out
> against chamber data?
```

Not yet, but this is planned. One of us (DT) works at the Forschungszentrum Jülich where the SAPHIR chamber is located. An investigation of the α- and β-pinene photooxidation by OH in the chamber has been presented very recently at the Atmospheric Chemical Mechanisms Conference in December 2018. MOM chemistry will be compared to these and other chamber results.

```
> How does it compare to other model aromatic atmospheric
> chemical mechanisms (the prediction of NO to NO2
> conversion and hence photochemical ozone formation, and
> chemical reactivity in various aromatics systems can vary
> significantly between different model chemistries.
```

This will be certainly an aspect of the mechanism evaluation that is intended in the future (see the reply above).

> Figure 1. Please list species by category i.e. alkanes,
> alkenes, aromatics, oxygenates etc

The figure has been rearranged as requested.

> Page 4. 2.1.1. VOC reactions with OH This section is
> severally lacking in detail with respect to the updates
> actually carried out and the impact of such updates.
> Specifically: When were the IUPAC rate constants last
> updated? Referencing the IUPAC website datasheets as
> Atkinson et al., (2006) is somewhat out of date.

Several rate constants have already been updated according to the IUPAC website in those cases where the Atkinson et al. (2006) has been superseeded. Detailed information for every reaction is already available in the file meccanism.pdf in the supplement. Here, the rate constants and references can be found for all MECCA reactions. Specifically, the citation "Wallington et al. (2018)" refers to the IUPAC website. It is shown whenever we are using an updated rate constant from the IUPAC website which is different from Atkinson et al. (2006).

> The updated substituent factors form the original SAR of
> Kwok and Atkinson need to be shown here (in a table) so
> that they can be compared/contrasted to other SAR
> approaches and so the methodology is transparent to the
> community.

We have added the new Table 1 to the manuscript which shows the updated values.

> "No rigorous evaluation of the SAR has been conducted and
> estimation uncertainty is expected to be in the same range
> as the MCM" I strongly recommend that an evaluation of the
> updated SAR is carried out and compared to the original
> and other SAR approaches used in other models/chemical
> mechanisms.

We acknowledge the crucial importance of such evaluation. However, we think is out of the scope of the present manuscript. We plan to assess and possibly adopt the recent SAR by Jenkin et al. (2018) in the evaluation of MOM against SAPHIR experiments for a range of VOC.

> Page 4. "2.1.2 RO2 reaction with NOx" Should be "with
> NOxy" as you also look at RO2 + NO3.

The name of the section has been changed to "RO_2 reactions with NO_x and NO_3".

> Page 7. 2.1.4 RO2 permutation reactions, Line 11 "The
> rate expressions are not from the MCM, except" The rate
> expressions "not from the MCM" need to be defined and put
> into a Table here.

We have added a new table (Table 2) with details concerning the rate constants for this reaction category. We also show the MCM values and relevant references.

> Page 7. 2.1.5 Photo-induced reactions Line 15 (and
> through-out) define photolysis rates as "j-values", i.e.
> j(NO2), and not "J-values" throughout.

We have changed to the lower-case notation as requested.

> Define "HPALD and "PACALD"

We define HPALD and PACALD as the conjugated unsaturated hydroperoxyenals from isoprene that have been originally proposed as the main source of OH recycling in isoprene chemistry. We have modified the text in section 2.1.5 accordingly.

> Figure 3 appears before it is mentioned in the text

The placement of the figures is indeed not correct yet. This will be corrected in collaboration with the Copernicus production office when the final two-column layout is produced.

> Page 8. 2.2 Other chemical mechanisms some discussions,
> even brief ones about differences in the chemical schemes,
> would be useful

The following text has been added: *"All mechanisms are suitable for stratospheric as well as tropospheric calculations. They all include the chemistry of chlorine and bromine, and they all include isoprene and terpenes. However, only MCM, MOM and JAM002 treat some terpenes individually, e.g., pinene. The JAM002 mechanism is larger than CB05BASCOE and MOZART but small compared to MECCA with MOM. The very detailed MCM is the largest of all. More information about the chemical mechanisms is provided in the following sections."*

> Again, some evidence of evaluation of the updated
> MECCA/MOM chemistry against older versions and other
> detailed chemical mechanisms (such as the MCM) is needed
> here.

As mentioned above, a comparison of MOM and MCM has been added to the text and to Fig. 3.

> Page 11, Table 1. Needs much more explanation here. What
> is the colour coding in the table?

The following text has been added: *"The color coding [...] shows in which mechanism a species occurs. For example, orange is used for species which are included in the full mechanism and in s1 but not in s2 and s3."*

> Page 10, line 11 "from a global atmospheric chemistry
> simulation based on", describe the scenarios used in this
> simulation

We assume the referee refers to page 12 here, not page 10.

We agree that a better description is needed how we obtained the 30 sample points from the global model simulation. The revised text is now:

"Sample points were extracted from a global atmospheric chemistry simulation with a setup similar to that presented by Lelieveld et al. (2016). The chemical compositions were taken from several boxes at two altitudes (at the surface and at about 1 km). As we want the skeletal mechanism to perform well not only at typical concentrations of the targets but also when they are very high or very low, we picked boxes where the targets reach their minimum, average, or maximum concentrations, respectively. This resulted in the generation of 30 sample points (5 targets times (min/ave/max) times 2 altitudes), covering a wide range of values."

> Page 15, Line 13 Figure 5 appears after the References?!

The placement of the figures will be done from scratch after the layout has been changed to the two-column format. We will then ensure that the figures occur at the correct positions.

> Page 16. 4 MECCA in the MESSy modelling system MESSy
> needs defining

We have now defined the acronym MESSy when it first occurs in the text, i.e., in the introduction.

> Page 20. Summary and outlook. Not actually a "summary" but
> a list of high level desirable goals. This should be
> re-written.

We admit that this section so far has been more "outlook" than "summary". We have added more text summarizing the new features of CAABA/MECCA.

References

Atkinson, R.: A structure-activity relationship for the estimation of rate constants for the gas-phase reactions of OH radicals with organic compounds, Int. J. Chem. Kinetics, 19, 799–828, doi:10.1002/kin.550190903, 1987.

Atkinson, R., Baulch, D. L., Cox, R. A., Crowley, J. N., Hampson, R. F., Hynes, R. G., Jenkin, M. E., Rossi, M. J., Troe, J., and IUPAC Subcommittee: Evaluated kinetic and photochemical data for atmospheric chemistry: Volume II – gas phase reactions of organic species, Atmos. Chem. Phys., 6, 3625–4055, doi:10.5194/ACP-6-3625-2006, 2006.

Cabrera-Perez, D., Taraborrelli, D., Sander, R., and Pozzer, A.: Global atmospheric budget of simple monocyclic aromatic compounds, Atmos. Chem. Phys., 16, 6931–6947, doi:10.5194/acp-16-6931-2016, 2016.

Crounse, J. D., Knap, H. C., Ørnsø, K. B., Jørgensen, S., Paulot, F., Kjaergaard, H. G., and Wennberg, P. O.: Atmospheric fate of methacrolein. 1. peroxy radical isomerization following addition of OH and O_2, J. Phys. Chem. A, 116, 5756–5762, doi:10.1021/jp211560u, 2012.

Jenkin, M. E., Valorso, R., Aumont, B., Rickard, A. R., and Wallington, T. J.: Estimation of rate coefficients and branching ratios for gas-phase reactions of OH with aliphatic organic compounds for use in automated mechanism construction, Atmos. Chem. Phys., 18, 9297–9328, doi:10.5194/acp-18-9297-2018, 2018.

Jöckel, P., Tost, H., Pozzer, A., Kunze, M., Kirner, O., Brenninkmeijer, C. A. M., Brinkop, S., Cai, D. S., Dyroff, C., Eckstein, J., Frank, F., Garny, H., Gottschaldt, K.-D., Graf, P., Grewe, V., Kerkweg, A., Kern, B., Matthes, S., Mertens, M., Meul, S., Neumaier, M., Nützel, M., Oberländer-Hayn, S., Ruhnke, R., Runde, T., Sander, R., Scharffe, D., and Zahn, A.: Earth System Chemistry integrated Modelling (ESCiMo) with the Modular Earth Submodel System (MESSy, version 2.51), Geosci. Model Dev., 9, 1153–1200, doi:10.5194/gmd-9-1153-2016, 2016.

Kwok, E. S. C. and Atkinson, R.: Estimation of hydroxyl radical reaction rate constants for gas-phase organic compounds using a structure-reactivity relationship: an update, Atmos. Environ., 29, 1685–1695, doi:10.1016/1352-2310(95)00069-B, 1995.

Lelieveld, J., Gromov, S., Pozzer, A., and Taraborrelli, D.: Global tropospheric hydroxyl distribution, budget and reactivity, Atmos. Chem. Phys., 16, 12 477–12 493, doi:10.5194/acp-16-12477-2016, 2016.

Mallik, C., Tomsche, L., Bourtsoukidis, E., Crowley, J. N., Derstroff, B., Fischer, H., Hafermann, S., Hüser, I., Javed, U., Keßel, S., Lelieveld, J., Martinez, M., Meusel, H., Novelli, A., Phillips, G. J., Pozzer, A., Reiffs, A., Sander, R., Taraborrelli, D., Sauvage, C., Schuladen, J., Su, H., Williams, J., and Harder,

H.: Oxidation processes in the eastern Mediterranean atmosphere: evidence from the modelling of HO_x measurements over Cyprus, Atmos. Chem. Phys., 18, 10 825–10 847, doi:10.5194/acp-18-10825-2018, 2018.

Taraborrelli, D., Lawrence, M. G., Crowley, J. N., Dillon, T. J., Gromov, S., Groß, C. B. M., Vereecken, L., and Lelieveld, J.: Hydroxyl radical buffered by isoprene oxidation over tropical forests, Nature Geosci., 5, 190–193, doi:10.1038/NGEO1405, 2012.

Wallington, T. J., Ammann, M., Cox, R. A., Crowley, J. N., Herrmann, H., Jenkin, M. E., McNeill, V., Mellouki, A., Rossi, M. J., and Troe, J.: IUPAC Task group on atmospheric chemical kinetic data evaluation: Evaluated kinetic data, URL http://iupac.pole-ether.fr, 2018.

The ~~atmospheric chemistry~~ community atmospheric-chemistry box model CAABA/MECCA-4.0

Rolf Sander[1], Andreas Baumgaertner[2], David ~~Cabrera~~Cabrera-Perez[1], Franziska Frank[3], Sergey Gromov[1,*], Jens-Uwe Grooß[4], Hartwig Harder[1], Vincent Huijnen[5], Patrick Jöckel[3], Vlassis A. Karydis[1,6], Kyle E. Niemeyer[7], Andrea Pozzer[1], Hella Riede[1,], Martin G. Schultz[6,***], Domenico Taraborrelli[6], and Sebastian Tauer[1]**

[1]Air Chemistry Department, Max-Planck Institute of Chemistry, P.O. Box 3060, 55020 Mainz, Germany
[2]Deutsches Zentrum für Luft- und Raumfahrt (DLR), Project Management Agency, 53227 Bonn, Germany
[3]Deutsches Zentrum für Luft- und Raumfahrt (DLR), Institut für Physik der Atmosphäre, Oberpfaffenhofen, 82234 Weßling, Germany
[4]IEK-7, Forschungszentrum Jülich, Jülich, Germany
[5]Royal Netherlands Meteorological Institute (KNMI), De Bilt, the Netherlands
[6]IEK-8, Forschungszentrum Jülich, Jülich, Germany
[7]School of Mechanical, Industrial & Manufacturing Engineering, Oregon State University, Corvallis, Oregon, USA
[*]also at: Institute of Global Climate and Ecology (Roshydromet and RAS), Moscow, Russia
[**]now at: Research and Development, Method Development in Remote Sensing, German Weather Service (DWD), Germany
[***]now at: Jülich Supercomputing Center (JSC), Forschungszentrum Jülich, Jülich, Germany

Correspondence: R. Sander (rolf.sander@mpic.de)

Abstract. We present version 4.0of the atmospheric chemistry box model CAABA/MECCA which now includes a number of new features: (i) skeletal mechanism reduction, (ii) the MOM chemical mechanism for volatile organic compounds, (iii) an option to include reactions from the Master Chemical Mechanism (MCM) and other chemical mechanisms, (iv) updated isotope tagging, and (v) improved and new photolysis modules (JVAL, RADJIMT, DISSOC). Further, when MECCA is connected to a global model, the new feature of coexisting multiple chemistry mechanisms (Poly-MECCA/CHEMGLUE) can be used. Additional changes have been implemented to make the code more user-friendly and to facilitate the analysis of the model results. Like earlier versions, CAABA/MECCA-4.0 is a community model published under the GNU General Public License.

1 Introduction

~~A full description of the multi-purpose atmospheric chemistry box model CAABA/~~MECCA (~~Chemistry As A Boxmodel Application/ M~~*M*odule ~~E~~*E*fficiently ~~C~~*C*alculating the ~~C~~*C*hemistry of the ~~Atmosphere)~~ *A*tmosphere) is an atmospheric chemistry module that contains a comprehensive chemical mechanism with tropospheric and stratospheric chemistry of both the gas and the aqueous phase. In addition to the basic HO_x, NO_x, and methane chemistry, it also includes non-methane hydrocarbons (NMHCs), halogens (Cl, Br, I), sulfur (S), and mercury (Hg) chemistry. For the numerical integration, MECCA uses the KPP software (Sandu and Sander, 2006).

To apply the MECCA chemistry to atmospheric conditions, MECCA must be connected to a base model via the MESSy (*M*odular *E*arth *S*ubmodel *Sy*stem) interface (Jöckel et al., 2010). This base model can be a complex, 3-dimensional model but it can also be a simple box model. CAABA (*C*hemistry *A*s *A* *B*oxmodel *A*pplication) is such a box model, simulating the atmospheric environment in which the MECCA chemistry takes place.

A full description of CAABA/MECCA has already been published elsewhere (Sander et al., 2005, 2011a). Here, we only present new features that have been implemented after version 3.0. Section 2 describes all changes related to the chemical mechanism of MECCA. In Sect. 3 we show several new options for calculating photolysis rate coefficients in the model.

~~Most of the recent MECCA developments can be used in the CAABA/MECCA model, which represents a single air parcel (i.e., a box) in the atmosphere. However, there are also additional features , which can be used~~ Section 4 presents new features which are only useful when MECCA is coupled to a global (3-dimensional) base model~~via the MESSy interface (Jöckel et al., 2010). These are discussed in Sect. 4~~.

2 The chemical mechanism MECCA

MECCA is a chemistry submodel that contains a comprehensive atmospheric reaction mechanism, including 1) the basic O_3, CH_4, HO_x, and NO_x chemistry, 2) non-methane hydrocarbon (NMHC) chemistry, 3) halogen (Cl, Br, I) chemistry, and 4) sulfur chemistry. Recent extensions of MECCA are presented in the following sections.

2.1 The Mainz Organic Mechanism (MOM)

The Mainz Organic Mechanism (MOM) is the default oxidation mechanism for volatile organic compounds (VOCs = CH_4 + NMHCs) in MECCA. The current MOM mechanism is a further development of the versions used by Lelieveld et al. (2016) and Cabrera-Perez et al. (2016). It includes developments from Taraborrelli et al. (2012), Hens et al. (2014), and Nölscher et al. (2014). MOM chemistry has been used by Mallik et al. (2018) to study oxidation processes in the Mediterranean atmosphere. Figure 1 shows all 43 primarily emitted species that are treated by MOM. These species are alkanes and alkenes up to four carbon atoms, ethyne (acetylene), two nitriles, isoprene, 2-methyl-3-buten-2-ol (MBO), five monoterpenes, and nine aromatics. Most of the oxidation scheme is explicit~~with a low degree of lumping~~. Lumping is used for some isomers with similar properties, e.g., the MOM species "LXYL" presents the sum of *o*-, *m*- and *p*-xylene. All lumped species are marked by the prefix "L" in their names. The full mechanism includes about 600 species and 1600 reactions. A list of all chemical reactions, including rate coefficients and references, is available in the supplement (meccanism.pdf).

The mechanism for the isoprene oxidation was developed starting from MIM2 (Taraborrelli et al., 2009), which is a reduction of ~~the~~ MCM v3.1 (Rickard and Pascoe, 2009; Jenkin et al., 1997). The major mechanisms, which regenerate OH under low-NO_x conditions are included. OH-addition to the unsaturated isoprene hydroperoxides has been implemented yielding entirely epoxydiols and OH according to Paulot et al. (2009). The *Z*-1,4- and *Z*-4,1-ISOPO2 isomers undergo 1,6-H-shifts as originally proposed by Peeters et al. (2009). In MOM the corresponding rate coefficients are those computed by Taraborrelli et al. (2012), and the 66% ~~HPALDs yields~~ yields of isoprene-derived hydroperoxyenals (HPALDs) are according to Nölscher et al. (2014). For the non-HPALD-yielding channel, the corre-

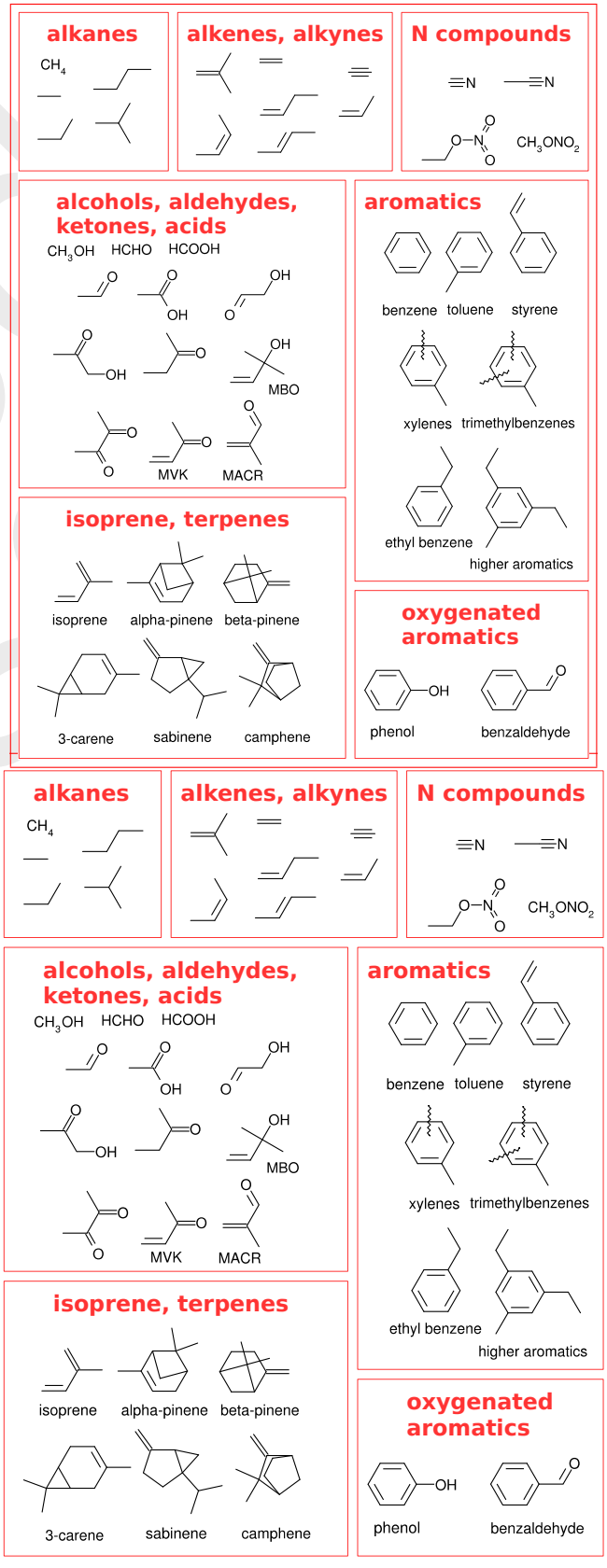

Figure 1. Primarily emitted species treated by MOM.

sponding mechanisms proposed by Peeters et al. (2014) and Jenkin et al. (2015) have been included, however, in a simplified manner. The estimated photo-induced cascade of reactions produces substantial amounts of OH (see Sect. 2.1.5). Finally, methacrolein (MACR) oxidation has been implemented according to Orlando et al. (1999), except for the fate of the methylvinyl radical. The rate of the 1,4-H-shift for the MACRO2 radical is ~~treated as predicted by Taraborrelli et al. (2012), which is about an order of magnitude lower than proposed~~ now calculated using the expression reported by Crounse et al. (2012).

Oxidation of the two important terpenes, α-pinene and β-pinene, is based on ~~the~~ MCM (Jenkin et al., 2000). However, important modifications following the theoretical work of L. Vereecken have been implemented with some simplifications (Vereecken et al., 2007; Nguyen et al., 2009; Vereecken and Peeters, 2012; Capouet et al., 2008). For instance, minor channels of the OH- and O_3-initiated oxidation are neglected.

Aromatics (benzene, toluene, xylenes) are oxidized in the mechanism by Cabrera-Perez et al. (2016), which is to large extent a reduction of the corresponding MCM ~~v3.3.1~~ (Jenkin et al., 2003; Bloss et al., 2005). Photolysis of ortho-nitrophenols yielding HONO has been added according to Bejan et al. (2006) and Chen et al. (2011). Finally, reactions of phenyl peroxy radicals with NO_2 yielding NO_3 have been added, consistent with Jagiella and Zabel (2007).

Oxidation of VOCs by O_3 and NO_3 is similar to that in ~~the~~ MCM. The oxidation by OH, however, significantly differs from ~~the~~ MCM treatment and therefore is detailed in the next section.

2.1.1 VOC ~~reaction~~ reactions with OH

Reactions of OH with organic molecules can be either H-abstraction or OH-addition. If available, experimental rate coefficients are preferred and taken mostly from the IUPAC kinetic data evaluation ~~(Atkinson et al., 2006)~~(Atkinson et al., 2006; Wallington et al., 2018). Unmeasured rate coefficients for the C_1 to C_5 species are estimated with a site-specific Structure-Activity Relationship (SAR) similar to ~~the~~ MCM, based on the work of Atkinson (1987) and Kwok and Atkinson (1995). The base rate coefficients for OH-addition to double bonds are taken from the more recent SAR by Peeters et al. (2007). For the C_6 to C_{11} closed-shell species, the MCM rate coefficients are retained. It is worth noting that the ~~latter~~ SAR-estimated ones have no temperature-dependence and are only given at 298 K. The effect of neighbouring groups is expressed by substituent factors and is differentiated by functional group. Most substituent factors by Kwok and Atkinson (1995) are updated or calculated *ex novo* by computing the relative rate coefficient of OH with the simplest VOC bearing the substituent relative to the one of its parent compound (Tab. 1). A clear limitation of this approach is that for OH-addition no substituent effect on the branching ratios is considered. No rigorous evaluation of the SAR has been conducted and the estimation uncertainty is expected to be in the same range as for the SAR used by ~~the~~ MCM.

The general formulae for H-abstraction by OH are:

$$k(CH_3X) = k_{\underline{p}p} \cdot F(X) \quad (1)$$

$$k(CH_2XY) = k_{\underline{s}s} \cdot F(X) \cdot F(Y) \quad (2)$$

$$k(CHXYZ) = k_{\underline{t}t} \cdot F(X) \cdot F(Y) \cdot F(Z) \quad (3)$$

where ~~k_p, k_s, k_t~~ k_{p}, k_{s}, k_{t} are the group rate coefficients for the hydrogens on the primary, secondary and tertiary carbon atoms, respectively, and $F(X)$ is the factor for the substituent X.

The SAR for OH-addition to (poly)alkenes is based on the hypothesis that the site-specific rate coefficient depends solely on the stability of the radical product (Peeters et al., 2007). Thus, rate coefficients for the formation of primary, secondary and tertiary radicals are derived from the high-pressure limits for ethene, 2-butene and 2,3-dimethyl-2-butene, respectively. It's worth noting that for the tertiary radical formation, Peeters et al. (2007) used solely the rate coefficient for 2,3-dimethyl-2-butene and not that for 2-methyl-2-butene minus that for the secondary radical.

2.1.2 RO_2 ~~reaction~~ reactions with NO_x and NO_3

Reactions with NO are the dominant sink for RO_2 under polluted conditions. The RO_2-size independent MCM rate coefficient is used with the exception of CH_3O_2 and $CH_3CH_2O_2$, for which the IUPAC recommendations are followed (Atkinson et al., 2006). In general, the two possible reaction channels are considered:

$$RO_2 + NO \rightarrow (1-\alpha) \times (RO + NO_2) \quad (R1)$$

$$\alpha \times RONO_2 \quad (R2)$$

with α being the alkyl nitrate yield for the formation of alkyl nitrates, which curb tropospheric ozone production. Acyl RO_2 do not form nitrates. The CH_3ONO_2-yield is calculated according to Butkovskaya et al. (2012) with a reduction according to Flocke et al. (1998). The $CH_3CH_2ONO_2$-yield is calculated according to Butkovskaya et al. (2010). For all other peroxy radicals the corresponding alkyl nitrate yields are calculated with the relationship by Arey et al. (2001), which depends on temperature, pressure and molecular size. However, the latter is represented not by the number of carbon atoms but by the number of heavy atoms (excluding the $-OO$ moiety) according to Teng et al. (2015). The oxygen atom in β-carbonyl RO_2 is not counted. Due to disagreement in the literature, no dependence of α on the degree of RO_2 substitution (primary, secondary and tertiary) is considered. Reduction factors for β- and γ-carbonyl RO_2 are derived from Praske et al. (2015) and for bicyclic RO_2 from aromatics are derived from Elrod (2011). As an example, Figure 2

Table 1. SAR parameters and substituent factors in MOM, largely based on Kwok and Atkinson (1995) for H-abstraction and on Peeters et al. (2007) for OH-addition, unless noted otherwise. Most base rate constants and substituent factors are updated with data from Atkinson et al. (2006). Original values for the substituent factors given by Kwok and Atkinson (1995) are listed in parentheses. All rate constants refer to reactions with OH.

		k for H-abstraction by OH in $\mathrm{cm^{-3}s^{-1}}$	
k_p	k_p (primary)	$4.49\times10^{-18}\times(T/\mathrm{K})^2\times\exp(-320\,\mathrm{K}/T)$	
k_s	k_s (secondary)	$4.50\times10^{-18}\times(T/\mathrm{K})^2\times\exp(253\,\mathrm{K}/T)$	
k_t	k_t (tertiary)[a]	$2.12\times10^{-18}\times(T/\mathrm{K})^2\times\exp(696\,\mathrm{K}/T)$	
k_rohro	k (hydroxylic)	$2.1\times10^{-18}\times(T/\mathrm{K})^2\times\exp(-85\,\mathrm{K}/T)$	
k_co2h	k (carboxylic)	$0.7\times4.0\times10^{-14}\times\exp(850\,\mathrm{K}/T)$	$=0.7\times k_{\mathrm{CH_3CO_2H}}$
k_roohro	k (hydroperoxidic)	$0.6\times5.3\times10^{-12}\times\exp(190\,\mathrm{K}/T)$	$=0.6\times k_{\mathrm{CH_3OOH}}$
		Substituent factors $F(X)$	
f_alk	$F(-\mathrm{CH_2}-)$	1.23 (1.23)	
f_alk	$F(>\mathrm{CH}-)$	1.23 (1.23)	
f_alk	$F(>\mathrm{C}<)$	1.23 (1.23)	
f_soh	$F^\mathrm{sec}(-\mathrm{OH})$	3.44 (3.50)	$(k_{\mathrm{CH_3CH_2OH}\rightarrow\mathrm{CH_3CHOH}})/k_\mathrm{s}$
f_toh	$F^\mathrm{tert}(-\mathrm{OH})$	2.68 (3.50)	$\frac{k_\text{2-propanol}-2k_\mathrm{p}-k_{\mathrm{ROH}\rightarrow\mathrm{RO}}}{k_\text{2-methylpropane}-3k_\mathrm{p}}$
f_sooh	$F^\mathrm{sec}(-\mathrm{OOH})$	8.00 (–)	$(k_{\mathrm{CH_3OOH}\rightarrow\mathrm{CH_2OOH}})/k_\mathrm{p}$
f_tooh	$F^\mathrm{tert}(-\mathrm{OOH})$	8.00 (–)	$(k_{\mathrm{CH_3OOH}\rightarrow\mathrm{CH_2OOH}})/k_\mathrm{p}$
f_ono2	$F(-\mathrm{ONO_2})$	0.04 (0.04)	
f_ch2ono2	$F(-\mathrm{CH_2ONO_2})$	0.20 (0.20)	
f_cpan	$F(-\mathrm{C(O)OONO_2})$	0.25 (–)	$(k_{\mathrm{CH_3C(O)OONO_2}})/k_\mathrm{p}$
f_allyl	$F^\mathrm{sec}(-\mathrm{allyl})$	3.6[b] (1.00)	$\frac{k_{\mathrm{CH_2CHCH_3}\rightarrow\mathrm{CH_2CHCH_2}}}{k_{\mathrm{CH_3CH_2CH_3}\rightarrow\mathrm{CH_3CH_2CH_2}}}$
f_cho	$F(-\mathrm{CHO})$	0.55 (0.75)	$\frac{k_{\mathrm{HOCH_2CHO}\rightarrow\mathrm{HOCHCHO}}}{k_\mathrm{p}F^\mathrm{sec}(-\mathrm{OH})}$
f_co2h	$F(-\mathrm{COOH})$	1.67 (0.74)	$(k_{\mathrm{CH_3COOH}\rightarrow\mathrm{CH_2COOH}})/k_\mathrm{p}$
f_co	$F(-\mathrm{C(=O)R})$	0.73 (0.75)	$(k_{\mathrm{CH_3CHO}\rightarrow\mathrm{CH_3CO}})/k_\mathrm{t}$
f_o	$F(=\mathrm{O})$	8.15 (8.70)	$(k_{\mathrm{CH_3CHO}\rightarrow\mathrm{CH_3CO}})/k_\mathrm{t}$
f_pch2oh	$F^\mathrm{prim}(-\mathrm{CH_2OH})$	1.29 (1.23)	$(k_{\mathrm{CH_3CH_2OH}\rightarrow\mathrm{CH_2CH_2OH}})/k_\mathrm{p}$
f_tch2oh	$F^\mathrm{tert}(-\mathrm{CH_2OH})$	0.53 (–)	$(k_{\mathrm{HOCH_2CHO}\rightarrow\mathrm{HOCH_2CO}})/(k_\mathrm{t}F(=\mathrm{O}))$
		k for OH-addition to double bonds in $\mathrm{cm^{-3}s^{-1}}$	
k_adp	k_adp (primary)	$4.5\times10^{-12}\times(T/300\,\mathrm{K})^{-0.85}$	$0.5k_{\mathrm{C_2H_4}}$ (high pressure limit)
k_ads	k_ads (secondary)	$1/4\times(1.1\times10^{-11}\times\exp(485\,\mathrm{K}/T)$ $+1.0\times10^{-11}\times\exp(553\,\mathrm{K}/T))$	$0.5k_\text{cis/trans-2-butene}$
k_adt	k_adt (tertiary)	$1.922\times10^{-11}\times\exp(450\,\mathrm{K}/T)-k_\mathrm{ads}$	$k_\text{2-methyl-2-butene}-k_\mathrm{ads}$
k_adsecprim		3.0×10^{-11}	$0.5(k_\text{1,3-butadiene}-2k_\mathrm{adp})$
k_adtertprim		5.7×10^{-11}	$0.5(k_\text{2,3-dimethyl-1,3-butadiene}-2k_\mathrm{adp})$
		Substituent factors $F_a(X)$	
a_pan	$F_a(-\mathrm{C(O)OONO_2})$	0.56 (–)	$k_\mathrm{MPAN}/k_\text{2-methylpropene}$
a_cho	$F_a(-\mathrm{CHO})$	0.31 (0.34)	$k^\mathrm{add}_\text{methacrolein}/k_\text{2-methylpropene}$
a_coch3	$F_a(-\mathrm{C(O)CH_3})$	0.76 (0.90)	$k_\mathrm{MVK}/k_\text{propene}$
a_ch2oh	$F_a(-\mathrm{CH_2OH})$	1.7 (1.6)	$k_\text{2-propene-1-ol}/k_\text{propene}$
a_ch2ooh	$F_a(-\mathrm{CH_2OOH})$	1.7 (–)	$k_\text{2-propene-1-ol}/k_\text{propene}$
a_coh	$F_a(>\mathrm{CHOH})$	2.2 (1.6)	$k_\text{1-pentene-3-ol}/k_\text{1-pentene}$
a_cooh	$F_a(>\mathrm{CHOOH})$	2.2 (1.6)	$k_\text{1-pentene-3-ol}/k_\text{1-pentene}$
a_co2h	$F_a(-\mathrm{C(O)OH})$	0.25 (0.25)	
a_ch2ono2	$F_a(-\mathrm{CH_2ONO_2})$	0.64 (0.47)	$\frac{k_{\mathrm{O_2NOCH_2C(CH_3)=CHCH_2OH}}}{F_a(-\mathrm{CH_2OH})k_\text{2-methyl-2-butene}}$

[a] There is a sign error in Kwok and Atkinson (1995) who present the value $\exp(-696\,\mathrm{K}/T)$ instead of $\exp(696\,\mathrm{K}/T)$.
[b] Median value from the range calculated by Vereecken and Peeters (2001).

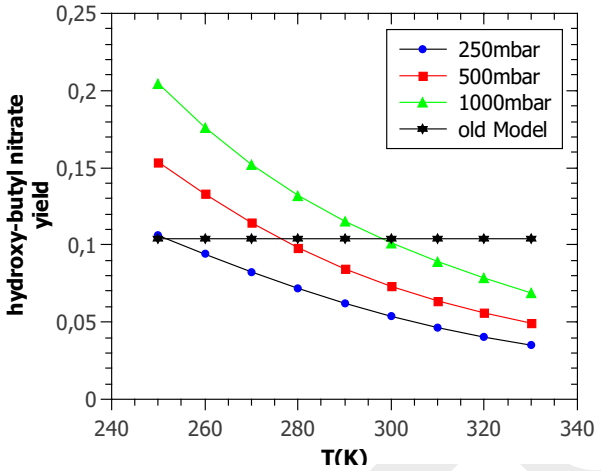

Figure 2. Temperature- and pressure-dependent nitrate yield for the secondary hydroxybutyl peroxy radical obtained calculated by MOM. ~~The~~ A constant yield of about 10 % ("old model") is used ~~in the~~ by MCM.

shows the predicted variable yield for the nitrate of the secondary hydroxy butyl peroxy radical.

Formation and decomposition of many peroxy nitrates is considered. The equilibria of acyl peroxy nitrates with their parent RO_2 are represented as in ~~the~~ MCM but the JPL kinetic data (Burkholder et al., 2015) is used. Only three alkyl peroxy nitrates, $CH_3O_2NO_2$, $CH_3CH_2O_2NO_2$ and $CH_3COCH_2O_2NO_2$, are represented. The equilibrium reactions for the latter are taken from Tyndall et al. (2001), Sehested et al. (1998) and Kirchner et al. (1999). Reactions of peroxy radicals with NO_3 all produce the corresponding alkoxy radical and NO_2:

$$RO_2 + NO_3 \rightarrow RO + NO_2 + O_2 \quad \text{(R3)}$$

The temperature-independent rate coefficient of $k(C_2H_5O_2 + NO_3) = 2.3 \times 10^{-12}\,cm^{-3}s^{-1}$ is used for all RCH_2O_2. For acyl peroxy radicals, an enhancement factor of $k(CH_3C(O)OO + NO_3)/k(C_2H_5O_2 + NO_3) = 1.74$ is calculated based on the peroxy acetyl radical.

2.1.3 RO_2 ~~reaction~~ reactions with HO_x

HO_2 reactions are often competitive with NO reactions of peroxy radicals. The former reactions are known to proceed via three channels

$$RO_2 + HO_2 \rightarrow RO + OH + O_2 \quad \text{(R4)}$$
$$ROOH + O_2 \quad \text{(R5)}$$
$$ROH + O_3 \quad \text{(R6)}$$

of which only the first is a radical propagating channel. Alkyl peroxy radicals cannot have the O_3-channel and their rate coefficient is calculated as a function of the number of carbons according to the fitting formula provided by Saunders et al. (2003) and Boyd et al. (2003). The branching ratios of the OH-channel for β-carbonyl, alkoxy and bicyclic peroxy radicals are taken from Dillon and Crowley (2008), Orlando and Tyndall (2012) and Birdsall et al. (2010), respectively. A 10 % OH-yield for reactions of β-hydroxyl peroxy radicals is taken from the isoprene oxidation study of Liu et al. (2013), which is consistent with the results of Groß (2013) and Paulot et al. (2009). The HO_2 reaction of the simplest acyl peroxy radical (CH_3CO_3) has unique branching ratios as determined by direct OH and O_3 measurements (Groß et al., 2014). For all other acyl peroxy radicals the kinetic data for β-hydroxy acyl peroxy radicals, e.g. $HOCH_2CO_3$, are taken from Groß (2013) with the rate coefficient having the temperature dependence as recommended by IUPAC.

There is laboratory evidence for a non-negligible reaction of CH_3O_2 with OH (Bossolasco et al., 2014):

$$CH_3O_2 + OH \rightarrow CH_3O + HO_2 \quad \text{(R7)}$$

The lower limit of the rate coefficient $1.4 \times 10^{-10}\,cm^{-3}s^{-1}$ reported by Bossolasco et al. (2014) is used in MOM. This is consistent with the revised experimental value by the same lab (Assaf et al., 2016). The major reaction channel involving HO_2 elimination represents (80 ± 20) % and is set as the only channel (Assaf et al., 2017). The other possible channels are very uncertain and are therefore not included.

2.1.4 RO_2 permutation reactions

The self and cross reactions of organic peroxy radicals are treated according to the permutation reaction formalism in ~~the~~ MCM (Jenkin et al., 1997). Every organic peroxy radical reacts in a pseudo-first-order reaction with a rate coefficient that is expressed as

$$k^{1st} = 2 \times \sqrt{k_{RO_2} \times k_{CH_3O_2}} \times [RO_2] \times \sqrt{k_{self,RO_2} \times k_{self,CH_3O_2}} \quad (4)$$

where ~~k_{self,RO_2}~~ k_{RO_2} = second-order rate coefficient of the self reaction of the organic peroxy radical, ~~k_{self,CH_3O_2}~~ $k_{CH_3O_2}$ = second-order rate coefficient of the self reaction of CH_3O_2, and $[RO_2]$ = sum of the concentrations of all organic peroxy radicals. The formalism is a simplification of the approach by Madronich and Calvert (1990) under the assumption that the dominant co-reactant of RO_2 is CH_3O_2. The value of ~~k_{self,CH_3O_2}~~ $k_{CH_3O_2}$ is taken from the IUPAC recommendations. Expressions for ~~k_{self,RO_2}~~ k_{RO_2} distinguish acyl from alkyl peroxy radicals. The latter are differentiated by the degree and kind of substituents close the $-OO$ moiety. The rate expressions (Tab. 2) are not from ~~the~~ MCM, except for β-hydroxyl radicals, and have a temperature dependence ~~(Atkinson et al., 2006; Glover and Miller, 2005; Orlando and Tynd~~

Table 2. Second-order rate constants k^{2nd} for permutation reactions (in $cm^{-3}s^{-1}$). Here, $k_{CH_3O_2} = 1.03E\text{-}13 \times \exp(365\,K/T)\,cm^{-3}s^{-1}$ is for the self-reaction of CH_3O_2.

variable	$k^{2nd} = 2 \times \sqrt{k_{RO_2} \times k_{CH_3O_2}}$	based on	reference
k_RO2RCO3	$2 \times 2E\text{-}12 \times \exp(500\,K/T)$	CH_3CO_3 + CH_3O_2	Atkinson et al. (2006)
	Alkyl radicals (unsubstituted, > C_3)		
k_RO2pRO2	$2 \times \sqrt{1E\text{-}12 \times k_{CH_3O_2}}$	RO_2 = $(CH_3)_2CHCH_2O_2$	Glover and Miller (2005)
k_RO2sRO2	$2 \times \sqrt{1.6E\text{-}12 \times \exp(-2200\,K/T) \times k_{CH_3O_2}}$	RO_2 = i-$C_3H_7O_2$	Orlando and Tyndall (2012)
k_RO2tRO2	$2 \times 3.8E\text{-}13 \times \exp(-1430\,K/T)$	t-$C_4H_9O_2$ + CH_3O_2	Wallington et al. (2018)
	Alkyl radical with either O or Cl in β		
k_RO2pORO2	$2 \times 7.5E\text{-}13 \times \exp(500\,K/T)$	$CH_3COCH_2O_2$ + CH_3O_2	Orlando and Tyndall (2012)
k_RO2sORO2	$2 \times \sqrt{7.7E\text{-}15 \times \exp(1330\,K/T) \times k_{CH_3O_2}}$	RO_2 = $CH_3CH(OH)CH(O_2)CH_3$	Orlando and Tyndall (2012)
k_RO2tORO2	$2 \times \sqrt{4.7E\text{-}13 \times \exp(-1420\,K/T) \times k_{CH_3O_2}}$	RO_2 = $(CH_3)_2C(OH)CO_2(CH_3)_2$	Orlando and Tyndall (2012)
	Allyl- and β-hydroxy alkyl radicals		
k_RO2LISOPACO2	$2 \times \sqrt{(2.8E\text{-}12 + 3.9E\text{-}12)/2 \times k_{CH_3O_2}}$	RO_2 = ISOPAO2 and ISOPCO2	Saunders et al. (2003)
k_RO2ISOPBO2	$2 \times \sqrt{6.9E\text{-}14 \times k_{CH_3O_2}}$	RO_2 = ISOPBO2	Saunders et al. (2003)
k_RO2ISOPDO2	$2 \times \sqrt{4.8E\text{-}12 \times k_{CH_3O_2}}$	RO_2 = ISOPDO2	Saunders et al. (2003)

2.1.5 Photo-induced reactions

The enhanced photolysis of carbonyl nitrates from isoprene is implemented according to Barnes et al. (1993) and Müller et al. (2014). The enhancement is applied to the ~~J~~photolysis rate coefficients (j-values) of nitrooxyacetone (NOA), nitrooxyacetaldehyde (NO3CH2CHO), lumped nitrates of methyl ethyl ketone (LMEKNO3), nitrates of MVK and MACR and unsaturated C_5-nitrooxyaldehyde from the isoprene + NO_3 reaction.

Keto-enol tautomerization of aldehydes induced by light absorption is implemented based on data for acetaldehyde (Clubb et al., 2012). The enols are in equilibrium with the corresponding aldehydes by HCOOH-catalysis (da Silva, 2010). Formic acid is then produced upon reaction of the enols with OH similarly to the simplest enol (So et al., 2014). Vinyl alcohol is also produced in the photolysis of propanal.

~~HPALD and PACALD photolysis~~ Photolysis of HPALDs is according to Peeters et al. (2014) and Jenkin et al. (2015) and the subsequent photolysis of the resulting carbonyl enols (HVMK and HMAC) is treated according to Nakanishi et al. (1977) and Messaadia et al. (2015).

Nitrophenols undergo photolysis yielding HONO, according to Bejan et al. (2006) and Chen et al. (2011), and assumed co-products being cyclic ketenes. However, the OH-formation channel (Cheng et al., 2009; Vereecken et al., 2016) is not implemented.

Conjugated unsaturated dialdehydes like butenedial and 2-methyl-butenedial from isoprene and aromatics oxidations undergo photolysis based on Xiang et al. (2007) and ~~the~~ MCM. Only the major channel, CO loss, is considered, and the ~~J~~j-values are scaled with ~~J~~$j(NO_2)$. The ketenes from photolysis of ~~PACALDs~~hydroperoxyacetyl conjugated unsaturated aldehydes from isoprene, conjugated unsaturated dialdehydes and nitrophenols undergo photo-dissociation yielding CO and an excited Criegee intermediate. The ~~J~~j-value is assumed to be the same as that for MVK with a unity quantum yield.

2.2 Other chemical mechanisms

In addition to the native chemistry mechanism of MECCA (available in the file gas.eqn), several other, independent mechanisms are now provided as well. ~~These are decribed~~ The chemical mechanisms CB05BASCOE and MOZART from the Copernicus Atmosphere Monitoring Service project (CAMS 42), and the Jülich Atmospheric Mechanism (JAM002) have been converted to KPP format and introduced into MECCA. It is also possible to use our previous, simple mechanism MIM1 (Jöckel et al., 2016). In addition, chemical mechanisms extracted and downloaded from the MCM web page can be converted with a script which makes them compatible with CAABA/MECCA. All mechanisms are suitable for stratospheric as well as tropospheric calculations. They all include the chemistry of chlorine and bromine, and they all include isoprene and terpenes. However, only MCM, MOM and JAM002 treat some terpenes individually, e.g., pinene. The JAM002 mechanism is larger than CB05BASCOE and MOZART but small compared to MECCA with MOM. The very detailed MCM is the largest of all. More information about the chemical mechanisms is provided in the following sections. ~~They can for example be used for~~

Having all mechanisms implemented in the same modeling system enables mechanism intercomparison studies ~~within the same CAABA box model~~under exactly the same conditions. This approach ensures that any resulting differences come from the chemical mechanism, not from any other parts of the model.

~~The chemical mechanisms~~ We have performed such an intercomparison for MOM, CB05BASCOE~~and MOZART from the Copernicus Atmosphere Monitoring Service project (CAMS 42) have been converted to KPP format and introduced into MECCA. Both mechanisms have been compared to MOM, and the initial results~~ , MOZART, MIM1, JAM002 and a comparable subset of MCM. Results are shown in Fig. 3.

~~In addition, the Jülich Atmospheric Mechanism (JAM002)is now also available within CAABA~~All mechanisms show a very similar decay of the initial isoprene. Terpenes are destroyed faster in the schemes which treat them as a lumped species (CB05BASCOE and MOZART). With respect to peroxyacetyl nitrate (PAN), especially CB05BASCOE shows very different values during the first day of the simulation. The calculated diurnal cycles of ozone, OH and NO_2 are similar for all mechanisms but their absolute values vary. Highest concentrations are produced by MIM1 and MCM, the lowest by CB05BASCOE and JAM002. MOM and MOZART are in between.

2.2.1 CB05BASCOE

The CB05BASCOE scheme (Huijnen et al., 2016) is a merge of a tropospheric and stratospheric chemistry scheme. The tropospheric chemistry is based on the Carbon Bond mechanism 2005 (CB05, Yarwood et al., 2005). Here, a lumping approach is adopted for organic species by defining a separate tracer species for specific types of functional groups. The scheme has been modified and extended to include an explicit treatment of C_1 to C_3 species (Williams et al., 2013), SO_2, dimethyl sulfide (DMS), methyl sulfonic acid (MSA) and ammonia (NH_3), as described by Huijnen et al. (2010). The reaction rates follow the recommendations given in either the JPL or IUPAC evaluation (Burkholder et al., 2015; Wallington et al., 2018). The stratospheric chemistry is based on that from the BASCOE (Belgian Assimilation System for Chemical ObsErvations) system (Errera et al., 2008) and is labelled "sb15b". This chemical scheme merges the reaction lists developed by Errera and Fonteyn (2001) to produce short-term analyses, with the list included in the SOCRATES 2-D model for long-term studies of the middle atmosphere (Brasseur et al., 2000; Chabrillat and Fonteyn, 2003). The list of species includes all the ozone-depleting substances and greenhouse gases necessary for multi-decadal simulations of the couplings between dynamics and chemistry in the stratosphere, as well as the reservoir and short-lived species necessary for a complete description of stratospheric ozone photochemistry. Gas-phase and heterogeneous reaction rates are taken from the JPL evaluations 17 and 18 (Sander et al., 2011b; Burkholder et al., 2015). The merged reaction mechanism includes 99 species interacting through 211 gas-phase and 10 heterogeneous reactions. Details regarding its implementation and evaluation within the ECMWF Integrated Forecasting System (IFS) are given by Huijnen et al. (2016).

2.2.2 MOZART

The tropospheric chemistry in MOZART is based on the MOZART-3 mechanism by Kinnison et al. (2007). It includes additional species and reactions from MOZART-4 (Emmons et al., 2010) and further updates from the Community Atmosphere Model with interactive chemistry, referred to as CAM4-chem (Lamarque et al., 2012). The chemical mechanism includes an updated isoprene oxidation scheme and a better treatment of volatile organic compounds, with lumped species to represent large alkanes, alkenes and aromatic compounds as well as their oxidation products. Overall, it includes the degradation of C_1, C_2, C_3, C_4, C_5, C_7, and C_{10} species. The heterogeneous chemistry in the troposphere is implemented according to the corresponding module from CB05BASCOE. MOZART includes the extended stratospheric chemistry discussed by Kinnison et al. (2007) with further updates from CAM4-chem (Lamarque et al., 2012; Tilmes et al., 2016). This includes detailed gas-phase halogen chemistry of chlorine and bromine. The stratospheric chemistry accounts for heterogeneous processes on liquid sulfate aerosols and polar stratospheric clouds, following the approach of Considine et al. (2000). Overall, the MOZART mechanism includes 117 gas-phase species, 65 photolysis and 247 gas-phase reactions. Rate coefficients are taken from the JPL recommendations (Sander et al., 2006, 2011b).

2.2.3 JAM002

Version 2 of the Jülich Atmospheric Mechanism (JAM002) has been implemented in the ECHAM-HAMMOZ chemistry-climate model (Schultz et al., 2018). It is a blend of the stratospheric chemistry scheme of the Whole Atmosphere Chemistry Climate Model (WACCM, Kinnison et al., 2007) and version 4 of the tropospheric Model of OZone And Related Tracers (MOZART, Emmons et al., 2010). The combined chemistry scheme of WACCM and MOZART has been enhanced with a detailed representation of the oxidation of isoprene following the Mainz Isoprene Mechanism 2 (MIM2, Taraborrelli et al., 2009), and by adding a few primary volatile organic compounds and their oxidation chains. The isoprene oxidation scheme includes recent discoveries of 1,6 H-shift reactions (Peeters et al., 2009), the formation of epoxide (Paulot et al., 2009) and the photolysis of ~~isoprene-derived hydroperoxyenals (HPALDs, Wolfe et al., 2012)~~HPALDs (Wolfe et al., 2012). Some of the reaction products and rates were taken from ~~the~~ MCM (Jenkin et al., 2015). Radical-radical reactions have been substantially revised since Emmons et al. (2010). In contrast to ~~the~~ MCM, JAM002 does not use a radical pool but instead follows the pathways of peroxy radical reactions with HO_2, CH_3O_2, and CH_3COO_2 (peroxy acetyl) as explicitly as possible. Inorganic tropospheric chemistry considers ozone, NO, NO_2, NO_3, N_2O_5, HONO, HNO_3,

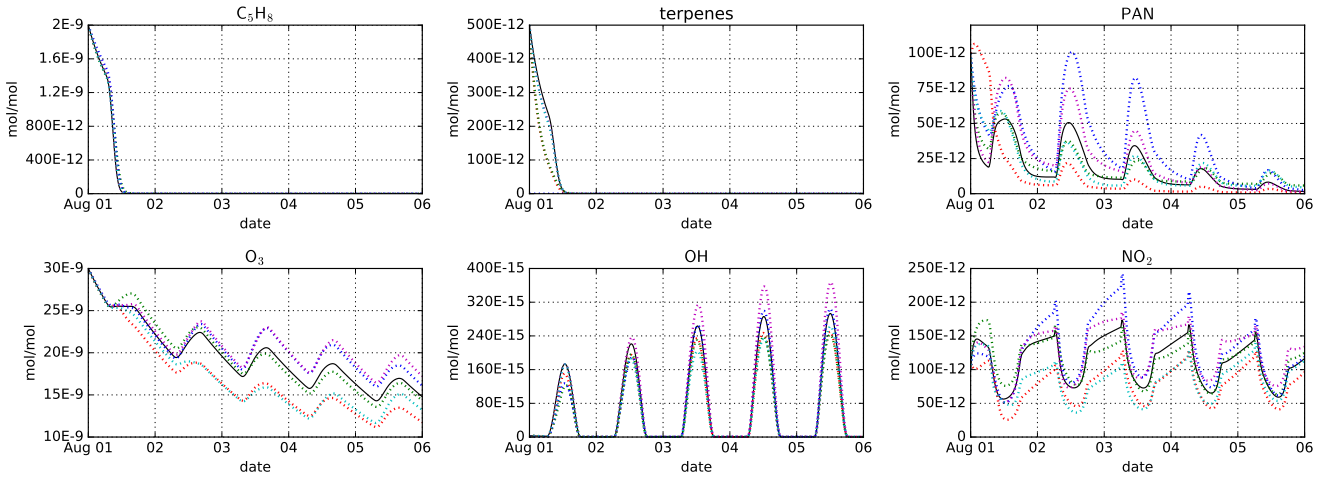

Figure 3. Intercomparison of the MOM (black), CB05BASCOE (red), ~~and~~ MOZART (green), MIM1 (blue), MCM (magenta), and JAM002 (cyan) mechanisms. The simulations represent the boundary layer over the Amazon forest. They start on 1 August at midnight and last for ~~10~~ 5 days. Temperature, pressure, and relative humidity are set to 301 K, 101325 Pa, and 70 %, respectively. The model is initialized with ~~100 pmol/mol PAN,~~ 2 nmol/mol isoprene (C_5H_8), ~~and~~ 500 pmol/mol of terpenes (α- and β-pinene, camphene, carene, and sabinene for MOM; lumped terpenes for CB05BASCOE and MOZART; not included in MIM2; α- and β-pinene for MCM and JAM002), and 100 pmol/mol PAN. During the model simulation, emissions of NO are set to 3.3×10^{-9} $cm^{-2}s^{-1}$ (Taraborrelli et al., 2009).

HNO_4, HCN, CO, H_2, OH, HO_2, H_2O_2, NH_3, chlorine and bromine species, SO_2, and oxygen atoms. The complete mechanism of JAM002 (species and equations) can be found in the directory mecca/eqn/jam/ in the supplement. In total, JAM002 contains 246 species and 733 reactions, including 142 photolysis reactions. Detailed information can be found in Schultz et al. (2018).

2.2.4 MCM

The Master Chemical Mechanism (MCM) describes in detail the tropospheric degradation of more than a hundred VOCs (Jenkin et al., 1997; Saunders et al., 2003). It is widely used as the reference mechanism for modeling studies of atmospheric processes. Although the standard organic chemistry mechanism in MECCA (MOM, described above) is sufficient for many model applications, a more explicit mechanism can be necessary when studying specific VOCs. For example, the fate of limonene ($C_{10}H_{16}$) emitted from boreal forests is not included in the standard MECCA mechanism. To use the MCM reactions inside MECCA, the new tool xmcm2mecca has been added, which converts an extracted subset ~~from the MCMweb page~~of MCM[1] to a KPP equation file that is compatible with MECCA. The User Manual provides a detailed description of this new tool.

[1]http://mcm.leeds.ac.uk/MCM

2.3 Skeletal mechanism reduction

In the area of fuel combustion research, chemical models require highly complex mechanisms to describe ignition, flame propagation, and other properties. In order to save computing time, several methods have been developed to create a simplified chemical mechanism (called skeletal mechanism), which still produces similar results as the full mechanism (e.g., Tomlin and Turányi, 2013). One of these methods is DRGEP (Directed Relation Graph with Error Propagation), which was introduced by Pepiot-Desjardins and Pitsch (2008) and implemented into the MARS (Mechanism Automatic Reduction Software) model by Niemeyer et al. (2010) and Niemeyer and Sung (2011). The DRGEP code from MARS has been implemented in CAABA/MECCA, making the skeletal reduction method available for atmospheric chemistry mechanisms. The most important quantities of DRGEP are briefly explained below, full details can be found in Niemeyer et al. (2010).

Targets: Important chemical species, for which the skeletal mechanism has to produce similar results as the full mechanism.

Sample points: A set of environmental conditions (temperature, pressure, concentrations of chemical species) simulated by the chemistry model.

Interaction coefficients (DIC, PIC, OIC): The importance of chemical species in a mechanism is defined in terms

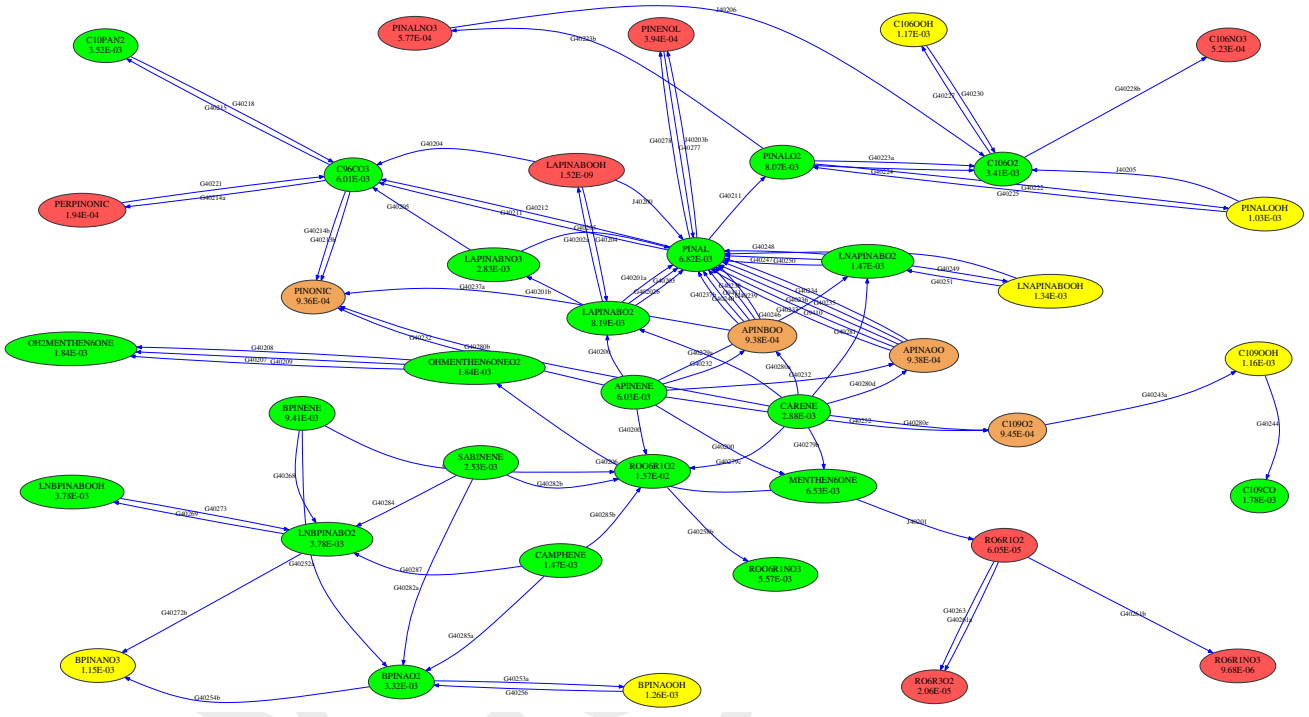

Figure 4. Skeletal reduction of terpene chemistry in the MOM reaction scheme (only C_{10} species are shown here). Vertex colors and OIC values correspond to those in Tab. 3: Only the green and yellow species are kept in the reduced mechanism.

of several interaction coefficients. The direct interaction coefficient (DIC) describes the importance of one species for another, based on its normalized contribution to production/consumption rates through reactions involving both species. Then, a graph search calculates a path interaction coefficient (PIC) based on the product of direct interaction coefficients along the path from target to species, where nodes represent species and weighted directed edges represent DICs. Finally, the overall interaction coefficient (OIC) is the maximum of all PICs between target and species. It is calculated for all sample points and expressed as a value between 0 (unimportant) and 1 (important). For ~~target species~~targets, OIC = 1 by definition. OIC values are only calculated for the full mechanism.

Error δ_{skel}: A normalized value describing the error when using a skeletal mechanism instead of the full mechanism. A skeletal mechanism is suitable if $\delta_{\mathrm{skel}} < 1$ for all targets and sample points. To allow individual weighting, the calculation of δ_{skel} depends on a target threshold AbsTol and a maximum acceptable relative tolerance RelTol, which are defined for all targets:

$$\delta_{\mathrm{skel}} = \left| \frac{\max(x_{\mathrm{skel}}, \mathrm{AbsTol})}{\max(x_{\mathrm{full}}, \mathrm{AbsTol})} - 1 \right| / \mathrm{RelTol} \qquad (5)$$

where x_{full} and x_{skel} are the mixing ratios calculated with the full and the skeletal mechanism, respectively.

OIC threshold $\varepsilon_{\mathrm{ep}}$: A chemical species is considered important if OIC(species) $> \varepsilon_{\mathrm{ep}}$. The final $\varepsilon_{\mathrm{ep}}$ calculated by DRGEP is the maximum value for which $\delta_{\mathrm{skel}} < 1$ still holds.

To test the skeletal mechanism generation, we chose HCHO, HO_2, NO, O_3, and OH as ~~target species~~targets, allowing a relative tolerance of RelTol = 20 % for mixing ratios above a threshold of AbsTol = 1 pmol/mol. ~~Thirty sample~~ Sample points were extracted from a global atmospheric chemistry simulation ~~based on Jöckel et al. (2016)~~with a setup similar to that presented by Lelieveld et al. (2016). The chemical compositions were taken from several boxes at two altitudes (at the surface and at about 1 km). As we want the skeletal mechanism to perform well not only at typical concentrations of the targets but also when they are very high or very low, we picked boxes where the targets reach their minimum, average, or maximum concentrations, respectively. This resulted in the generation of 30 sample points (5 targets times (min/ave/max) times 2 altitudes), covering a wide range of values~~for the target species~~. The full mechanism contained the complete set of species from MOM (Sect. 2.1).

Table 3. Simplified example list of species with overall interaction coefficients (OICs). The full mechanism includes all species; the skeletal mechanisms s1, s2, and s3 only include species above a certain OIC threshold. ~~Target species~~ Targets with OIC = 1 are always included. The color coding of the skeletal mechanism ~~is~~ (used also in Fig. 4) shows in which mechanism a species occurs. For example, orange is used for species which are included in the full mechanism and in s1 but not in s2 and s3.

species	OIC	full	s1	s2	s3
N	0.000000E+00	●			
PERPINONIC	1.944015E−04	●			
PINENOL	3.939767E−04	●			
PINALNO3	5.772079E−04	●			
PINONIC	9.361802E−04	●	●		
APINAOO	9.383650E−04	●	●		
APINBOO	9.383650E−04	●	●		
PINALOOH	1.033250E−03	●	●	●	
BPINANO3	1.147639E−03	●	●	●	
BPINAOOH	1.260848E−03	●	●	●	
MEK	1.282217E−03	●	●	●	
CAMPHENE	1.473224E−03	●	●	●	●
SABINENE	2.525735E−03	●	●	●	●
CARENE	2.877949E−03	●	●	●	●
APINENE	6.029040E−03	●	●	●	●
BPINENE	9.412960E−03	●	●	●	●
C5H8	2.914117E−01	●	●	●	●
MVK	3.432776E−01	●	●	●	●
PAN	3.505309E−01	●	●	●	●
CH4	5.527123E−01	●	●	●	●
NO2	9.998463E−01	●	●	●	●
HCHO	1.000000E+00	●	●	●	●
HO2	1.000000E+00	●	●	●	●
NO	1.000000E+00	●	●	●	●
O3	1.000000E+00	●	●	●	●
OH	1.000000E+00	●	●	●	●

To illustrate the mechanism, the subset describing terpene chemistry is shown in Fig. 4. The importance (OIC values) of a few selected species is shown in Tab. 3. Three skeletal mechanisms (s1, s2, s3) were generated, reducing the number of species from 663 in the full mechanism to 462, 429, and 411, respectively. The number of reactions was reduced from 2091 to 1444, 1320, and 1262, respectively. The third skeletal mechanism (s3) was rejected because it did not fulfill the criterion $\delta_{\mathrm{skel}} < 1$. Results obtained with the full mechanism and with s2 were compared in a global simulation, as described below in Sect. 4.2.

2.4 Kinetic and isotope tagging

We have updated the sub-submodel MECCA-TAG (Gromov et al., 2010), which had been introduced in version 3.0 of CAABA. Several improvements to the kinetic tagging technique were implemented. These new features include:

- Selectable composition transfer mode: Depending on the research question, prescribed-, molecular- or element-weighted composition transfer may be selected. These modes determine the shares with which each reactant contributes to the products in the tagged chemical reactions: according to user-specified weightings, proportional to the reacting molecules count, or following the given element (e.g., C or H) content, respectively. Whilst the latter mode is intrinsic to isotope tagging, the others may be used for custom tagging configurations, e.g., product yield calculations.

- Diagnostics for unaccounted production or loss of elemental composition: MECCA-TAG optionally adds passive diagnostic species to the tagged reactions with unbalanced transfer of the element of interest. This helps to quantify the amount of atoms the chemical mechanism receives from or loses to "nothing", including the isotope composition of such mass-balance violations.

- The new "class shifting" tagging mode: This mode allows migration of molecules between the tagging classes in specified reactions, which allows quantifying various exchange processes in the mechanism. For instance, one can distinguish oxidation generations: in reactions with given oxidants the products become "promoted" to the tagging class of the next oxidation generation. Another application of "class shifting" is quantifying the efficiency of recycling chains. In essence, such is the "online" implementation of the approach similar to that of Lehmann (2004), with the number of tagging classes defining the maximum of the recycling sequences it is possible to follow.

The range of MECCA-TAG applications was extended with new tagging setups/configurations:

- Radiocarbon configurations, which facilitate simulating the ^{14}C content in a desired set of species, including the routines for calculating abundances using conventional units like pMC (percent Modern Carbon).

- Hydrogen isotope chemistry: Now MECCA-TAG allows tracing pathways of H transfer between the species in the mechanism. Furthermore, D/H isotope chemistry (including relevant kinetic isotope effects for HO_x and $C_1 - C_2$ chemistry) are included. The configuration and calculations of the composition transfer were extended with the possibility to specify isotope branching ratios necessary for the consistent D/H kinetics simulations. Both H transfer and D/H chemistry are currently evaluated in stratospheric setups of CAABA (Frank et al., 2018).

- O_2 clumped isotope chemistry: simulation of non-stochastic distributions of $^{18}O^{18}O$ and $^{17}O^{18}O$

isotopologues (Δ_{36} and Δ_{35} signatures) resulting from $O(^3P)$-mediated temperature-dependent isotope exchange kinetics.

There are also some changes in the implementation and software requirements. There is no "doubling" mode anymore for evaluating the results of the optimized tagging. Performing kinetic tagging of the chemical mechanism with MECCA-TAG requires the Free Pascal Compiler (fpc[2], version ≥ 2.6) at the time the xmecca script is run. The submodel files are located in the mecca/tag/ directory of the distribution. The directory mecca/tag/cfg/ contains tagging configuration control files (*.cfg). The option to tag a newly created chemical mechanism is available in the xmecca script (also via batch files). Further details about the MECCA-TAG code development can be found in the file mecca/tag/CHANGELOG within the CAABA distribution.

3 Photolysis

CAABA contains several submodels which provide photolysis rate coefficients ~~J~~j, also called "~~J~~j-values". The simple submodels READJ and SAPPHO have already been described by Sander et al. (2011a). READJ has not changed since version 3.0. SAPPHO photolysis rates can now be scaled using a common enhancement factor "efact" for all photolysis rates. This has for instance been used to simulate the very bright conditions within a cloud top (Heue et al., 2014). The updated and new photolysis submodels JVAL and RADJIMT are described in the sections below.

3.1 JVAL

The submodel JVAL inside the CAABA/MECCA model calculates ~~J~~j-values using the method of Landgraf and Crutzen (1998). It was first updated to the version described by Sander et al. (2014), and then additional changes were made. Many new photolysis reactions have been added, most of them related to either species from the MOM mechanism (CH3NO3, CH3O2NO2, CH3ONO, CH3O2, HCOOH, C2H5NO3, NOA, MEKNO3, BENZAL, HOC6H4NO2, CH3COCO2H, IPRCHO2HCO, C2H5CHO2HCO, C3H7CHO2HCO, PeDIONE24, PINAL2HCO) or organic halogen compounds (CF2ClCFCl2, CH3CFCl2, CF3CF2Cl, CF2ClCF2Cl, CHF2Cl, CHCl3, CH2Cl2). Besides, bugfixes were necessary regarding incorrect temperature dependencies of the ozone and OCS cross sections in the input data.

3.2 RADJIMT

RADJIMT is a new submodel that provides dissociation and ionization rates due to absorption of light and energetic photoelectrons in the mesosphere and thermosphere (see Tab. 4).

[2]https://www.freepascal.org/

Table 4. New upper atmosphere reactions for which RADJIMT provides ~~J~~j-values.

$O(^3P)$	$+ e^*$	$\rightarrow$	$O^+ + e^- + e^*$
O_2	$+ e^*$	$\rightarrow$	$O_2^+ + e^- + e^*$
O_2	$+ e^*$	$\rightarrow$	$O^+ + O(^3P) + e^- + e^*$
N_2	$+ e^*$	$\rightarrow$	$N_2^+ + e^- + e^*$
N_2	$+ e^*$	$\rightarrow$	$N^+ + N + e^- + e^*$
N_2	$+ e^*$	$\rightarrow$	$N^+ + N(^2D) + e^- + e^*$
N_2	$+ e^*$	$\rightarrow$	$N + N(^2D) + e^*$
O_2	$+ h\nu$	$\rightarrow$	$O(^3P) + O(^1D)$
O_2	$+ h\nu$	$\rightarrow$	$O_2^+ + e^-$
O_2	$+ h\nu$	$\rightarrow$	$O^+ + O(^3P) + e^-$
$O(^3P)$	$+ h\nu$	$\rightarrow$	$O^+ + e^-$
H_2O	$+ h\nu$	$\rightarrow$	$H_2 + O(^1D)$
N_2	$+ h\nu$	$\rightarrow$	$N_2^+ + e^-$
N_2	$+ h\nu$	$\rightarrow$	$N^+ + N + e^-$
N_2	$+ h\nu$	$\rightarrow$	$N^+ + N(^2D) + e^-$
N_2	$+ h\nu$	$\rightarrow$	$N + N(^2D)$
NO	$+ h\nu$	$\rightarrow$	$NO^+ + e^-$

It is part of the upper atmosphere extension of MESSy initially described by Baumgaertner et al. (2013), which was partly based on the implementations from the middle and upper atmosphere model CMAT2 (Harris, 2001; Dobbin, 2005; Dobbin and Aylward, 2008). For upper atmosphere simulations with CAABA, MECCA was extended by the relevant chemical species (electrons and ions) and reactions (labeled %Up in gas.eqn). For the respective literature sources, see meccanism.pdf in the supplement.

Photodissociation and photoionization due to the absorption of solar X-ray, EUV, and UV radiation are calculated using fluxes from the SOLAR2000 empirical model (Tobiska et al., 2000), the GLOW model (Solomon et al., 1988), as well as data presented by Henke et al. (1993) and Fennelly and Torr (1992). Relative partitioning between the possible products of the ionization process are based on the model of Strickland and Meier (1982) and Fuller-Rowell (1993).

For solar zenith angles larger than 75°, the atmospheric column of each absorbing species is calculated using an approximation of the Chapman grazing incidence function (Smith and Smith, 1972).

Reaction enthalpies in kJ/mol (exothermic chemical heating) are provided as a product of the relevant chemical reactions when "set enthalpy=y" is defined in the MECCA batch file. Radiative heating and cooling is also calculated by the submodel (variable "heatrates").

As an example, we have performed simulations with CAABA using the MECCA and RADJIMT submodels. The mechanism was created using the batch file mtchem.bat, which selects reactions of the upper atmosphere labeled %Up. The model setup in caaba_mtchem.nml was used: The temperature was kept constant at 195 K, and the pressure was set to 0.5 Pa (approximately 85 km). The model starts on 1 January. Chemical species were initiliased us-

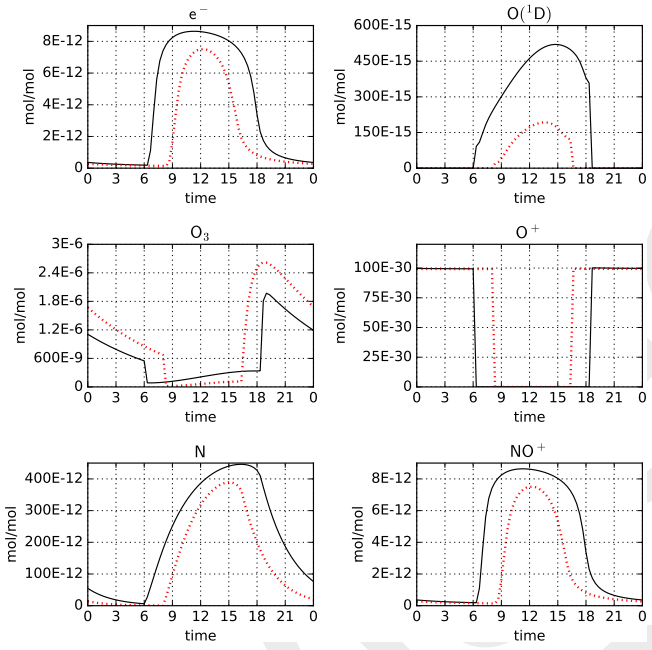

Figure 5. Model-calculated mixing ratios from an upper atmosphere simulation with MECCA and RADJIMT: Diurnal cycles for 4 January (after 3 days of spinup) for the equator (black) and a latitude of 50° N (red). Time is in hours, with local noon at 12. See Sect. 3.2 for further details.

ing the values provided by Brasseur and Solomon (2005) in their Tables A.6.1 and A.6.2. The default timestep length of 20 minutes was used. For MECCA and RADJIMT, the default settings were used. Model-calculated mixing ratios for a few selected species are shown in Fig. 5. A comprehensive set of plots is available in radjimt_mixrat.pdf and radjimt_jvalues.pdf in the supplement.

3.3 DISSOC

The new MESSy submodel DISSOC is based on the photolysis scheme by Meier et al. (1982). Briefly, it calculates a table of the so-called enhancement factor, which is basically the ratio of the actinic flux at a specific location to the solar irradiance at the top of the atmosphere. The enhancement factor depends on the pressure level, solar zenith angle and wavelength. Input data are the solar irradiance at the top of the atmosphere, absorption cross sections, ozone and oxygen profiles. For the implementation into global models, the input profiles are allowed to be latitude-dependent, which increases the dimensions of the enhancement factor table from three to four. Photolysis rates are calculated from the tabulated enhancement factor as a wavelength integral over the product with the absorption cross sections. The calculation is formulated in spherical geometry, such that it can be also applied to zenith angles above 90°. Rayleigh scattering is calculated based on Nicolet et al. (1982). Absorption cross sections are taken from the current JPL recommendations (Burkholder et al., 2015).

The code was first implemented by Lary and Pyle (1991) and coupled to a stratospheric chemistry-box model (Müller et al., 1994). Becker et al. (2000) improved the treatment of the diffuse actinic flux and corrected an implementation error of Meier et al. (1982). The extension to the use of multiple latitudes was introduced within the development of the model CLaMS (McKenna et al., 2002). The possibility to calculate diurnally averaged photolysis rates was introduced for the simplified fast chemistry setup used in multi-annual CLaMS simulations (Pommrich et al., 2014).

In the current configuration, DISSOC determines the photolysis rates for 38 photolysis reactions that are primarily of relevance in stratopsheric chemistry. A standard setup contains 36 pressure levels, 18 latitude bins, and 28 solar zenith angle bins (of which 8 are above 90°). Of the 203 standard wavelength intervals between 116 nm and 850 nm, typically only the 159 intervals above 175 nm are used for tropospheric and stratospheric applications.

4 MECCA in the MESSy modeling system

Apart from using MECCA inside the CAABA box model, it is also possible to connect MECCA chemistry to a trajectory or global, 3-dimensional model via the MESSy infrastructure (Jöckel et al., 2010, 2016). Recent developments of MECCA shown in this section are related to its implementation inside MESSy.

4.1 TRAJECT

The TRAJECT submodel by Riede et al. (2009) allows simulations of atmospheric chemistry along pre-calculated Lagrangian trajectories. For this purpose, the air parcel simulated by CAABA is moved through space and time along a trajectory taken from an external input file, while simulating atmospheric photochemistry with MECCA and JVAL. More generally, TRAJECT allows to prescribe physical boundary conditions for CAABA box model simulations. A typical application is the simulation of atmospheric trajectories (balloon measurements or backward trajectories). However, laboratory conditions (e.g., in a flow reactor) can also be prescribed. The previous TRAJECT version, described by Sander et al. (2011a), has been updated. The output is now more consistent with the trajectory input file, as physical information is now written out beginning with the first time step instead of the second. In general, an integration time step of chemical kinetics is always performed with the physical parameters given for the end of the time step. In that way, the mixing ratios written out at the end of a time step are consistent with the physical conditions at that point. Also, solar zenith angle and local time at the end of a time step are now

consistent with the given longitude and latitude for that trajectory point.

In addition to the trajectory input file, an external input file with ~~J~~j-values for NO_2 can be used to scale all ~~J~~j-values with the factor:

$$\text{jfac} = \frac{J(NO_2,\text{external})}{J(NO_2,\text{JVAL})} \frac{j(NO_2,\text{external})}{j(NO_2,\text{JVAL})} \quad (6)$$

To facilitate the analysis of the scaling impact, jfac is now written to output. Scaling thresholds have been implemented to prevent artifacts that would occur when ~~$J(NO_2,\text{JVAL})$~~ $j(NO_2,\text{JVAL})$ is very small and the calculation of jfac approaches a division by zero.

4.2 PolyMECCA/CHEMGLUE

In a standard global model simulation, the MESSy submodel MECCA contains one chemical mechanism that is used for all grid boxes. This ensures a consistent chemistry simulation from the surface to the upper atmosphere. However, in some cases, it may be preferable to allow different mechanisms in different boxes, e.g., terpene chemistry only in the troposphere and ion chemistry only in the mesosphere.

With the script xpolymecca, several independent chemical MECCA mechanisms can be produced. The first mechanism has the name "mecca", as usual. Additional mechanisms are labeled with a three-digit suffix. For example, the code of mechanism 2 is contained in messy_mecca002_kpp.f90 and related files.

To select an appropriate mechanism at each point in space and time, the MESSy submodel CHEMGLUE has been written. The name of the submodel was chosen because CHEMGLUE can also "glue" together different chemical mechanisms at the border where a chemical species is included in one mechanism but not in the other. CHEMGLUE defines the new channel object "meccanum", which contains the mechanism number for each grid point. These values can either be selected statically, e.g., depending on the model level number or the sea-land fraction mask. Alternatively, a dynamic (time-dependent) selection based on chemical or meteorological variables is possible, e.g., pressure, temperature, or the concentrations of ozone or isoprene.

Note that even when different boxes of a global model simulation use different chemistry mechanisms, the set of tracers contains all species from all mechanisms for all boxes.

The implementation ensures binary identical results when one chemical mechanism ("mecca") is replaced by two identical copies of it ("mecca" and "mecca002").

For a more realistic test, we created two different chemical mechanisms for organics. In the first mechanism, only the oxidation of methane is considered, and all non-methane hydrocarbons are neglected. The second (FULL) contains the full set of MOM (Sect. 2.1) reactions. CHEMGLUE selects the second mechanism whenever the mixing ratios of organics are above a threshold (isoprene $>$ 100 pmol/mol, α-pinene $>$ 100 pmol/mol, or toluene $>$ 10 pmol/mol). To investigate how much CPU time can be saved and how much the simplification affects the results, we have performed global test simulations based on the ECHAM5/MESSy atmospheric chemistry (EMAC) model by Jöckel et al. (2016). The horizontal resolution was T42 ($2.8° \times 2.8°$), with 47 vertical levels. Starting on 1 Jan 2009, one month was simulated. To facilitate the intercomparison between the simulations, the feedback of chemistry on the meteorology was switched off. Three different chemical scheme were tested:

1. FULL: Full MOM chemistry was activated throughout the atmosphere.
2. POLY: PolyMECCA/CHEMGLUE switches between the full MOM chemistry and the methane-only chemistry as described above.
3. SKEL: The skeletal mechanism s2 as described in Sect. 2.3 was activated throughout the atmosphere.

The CPU usage for the POLY and SKEL simulations are 62 % and 65 % of the FULL simulation, respectively. Results are shown in Fig. 6. Overall, the agreement between the simulations is quite good, considering that the simplified mechanisms neglect many reactions.

4.3 CHEMPROP

Chemical properties of the species in the reaction mechanism are needed at many locations in the model, e.g., molar mass (M), Henry's law constants (H), accommodation coefficients (α), acidity constants (K_A), and ion charge number (z). These values have so far been stored at different locations in the code (gas.tex, messy_cmn_gasaq.f90, and elsewhere). Because maintaining data that are spread over several source files is tedious and error-prone, the new CHEMPROP database has been created, which stores all values centrally in the ASCII table messy_main_tracer_chemprop.tbl. MECCA (and other submodels) can access these chemical property data via MESSy tracer containers, as described by Jöckel et al. (2008).

5 Further changes

- The new subroutines dilute and dilute_once dilute the concentrations of chemicals in an air parcel by mixing it with unperturbed air. This can for example be used for modeling chemistry in an expanding volcanic or smog plume. An alternative usage for these subroutines is the simulation of the flow in and out of a reaction chamber (e.g., van Eijck et al., 2013).
- A new functionality has been implemented for the external initialization of chemical species from a netCDF file: If the time axis of the input file contains more than

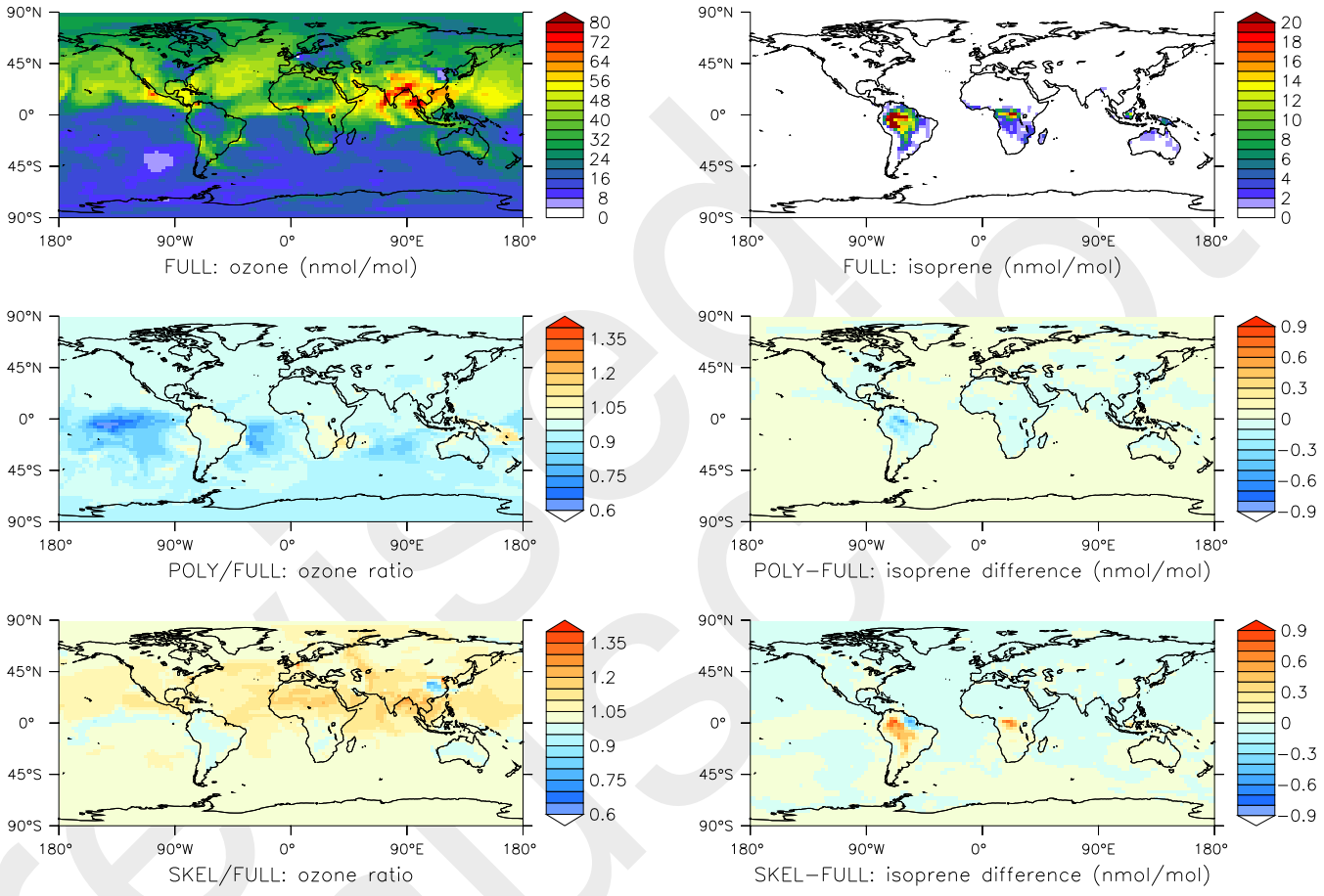

Figure 6. Results of the global comparison between the FULL, POLY, and SKEL mechanisms (see Sect. 4.2 for details). Shown are suface mixing ratios of ozone (left column) and isoprene (right column) at the end of the simulation, i.e. after one month. The top row shows results obtained with the FULL chemistry mechanism. The middle row compares POLY to FULL, and the bottom row compares SKEL to FULL.

one point, the time values are used to interpolate mixing ratios at model start time. This is convenient for bundling several initializations into one file, for instance to initialize several CAABA simulations from different points along a trajectory with recorded mixing ratios (see also Sect. 4.1). If the time axis of the input file contains only one point, the mixing ratios are read into CAABA, regardless of the time value.

– We extended CAABA with parameters to optionally control the output step frequency (output_step_freq) and the output synchronization frequency (output_sync_freq). The first variable sets the frequency at which values are written to the output. A value of output_step_freq $= \alpha$ skips $\alpha - 1$ timesteps and writes only every α-th time step to the output file. The second variable controls the output synchronization. Data are buffered for output_sync_freq time steps before they are written to the output files. Both parameters enable the user to carry out very long box model simulations without being constrained by machine I/O performance, and they can individually regulate the output file size. A high value of output_sync_freq has a positive effect on performance. However, in case of machine failure buffered output steps are lost.

– The treatment of humidity has been improved. Now specific as well as relative humidity (RH) are available throughout CAABA, and can be interconverted with generic conversion functions. Of the two, specific humidity is the more robust variable for humidity because the definition of RH can be based on either partial pressure or on specific humidity (Jacobson, 1999). There are various parameterizations for saturation water vapor pressure, and RH can be defined over liquid surface even below 0 °C, if supercooling is allowed. Functions that use humidity as input (concentration of air, conversion between humidity and water vapor concentration) now use the unambiguous specific humidity. If neces-

sary, it is derived from relative humidity taking all of the above considerations into account.

- For better model time control, two boolean namelist parameters have been introduced: l_groundhogday=T repeats a diurnal cycle while l_freezetime=T repeats a certain point in time, effectively freezing the solar zenith angle.

- The selection of various chemical species to define steady state has been simplified to allow for more flexibility in the criteria. The progress towards the defined steady state is now logged during CAABA runtime. Artifacts by species' concentrations close to zero are now prevented.

- ~~The previous script performing multiple model simulations (Sander et al., 2011a) has~~ Several shell scripts have been converted to python (xcaaba.py, multirun.py~~). It does not~~ , montecarlo.py). They use the netcdf4 interface and don't depend on the availability of the NetCDF operators (ncks etc.) anymore. Currently, the python scripts are in beta-testing. In future versions, they will replace the current tcsh scripts.

- Model results can now be visualized with ~~python scripts~~ the python script caabaplot.py using matplotlib. The previously used ferret scripts are still included but not actively supported anymore.

- Complex reaction mechanism can be interpreted as graphs, with species representing vertices and reactions representing edges. To visualize and analyze these graphs, the graph-tool software by Peixoto (2014) can now be used. For example, Fig. 4 was created with graph-tool.

- Rate coefficients have been updated to the latest JPL recommendations (Burkholder et al., 2015) and recent laboratory studies. A complete list of chemical reactions, rate coefficients, and references is available in the supplement (meccanism.pdf).

- The kinetic preprocessor KPP (Sandu and Sander, 2006) performs the numerical integration of the chemical reaction mechanism. It has been updated to the latest version 2.2.3, which contains a number of small fixes throughout the code[3].

- The scripts check_eqntags.py and check_eqns.pl check the internal consistency of the chemical mechanism.

- Details of all new features have been added to the updated User Manual, which now also includes an index. Additional minor bug fixes can be found in the CHANGELOG file.

[3] http://people.cs.vt.edu/~asandu/Software/Kpp

6 Summary and outlook

We have presented the current version of the atmospheric chemistry module MECCA-4.0, which includes several new features: Skeletal mechanism reduction, the MOM chemical mechanism for organic compounds, optional inclusion of reactions from MCM and other chemical mechanisms, updated isotope tagging, and improved and new photolysis modules. When MECCA is connected to a global model, PolyMECCA and CHEMGLUE allow coexisting multiple chemistry mechanisms. CAABA/MECCA is now available to the research community.

Based on the model development described in this paper, our current and upcoming goals are (for work in progress, initials of the principal investigators are shown in parentheses):

- Reduce complex mechanisms to a size suitable for global model simulations ~~.~~ (RS, KN).

- Perform a ~~chemical mechanism intercomparison for MOM,~~ chemistry module intercomparison including CB05BASCOE ~~, MOZART , JAM002, and the MCM~~and MOZART within a global chemistry modeling framework (Huijnen et al., 2019).

- Evaluate MOM chemistry and its effect on secondary aerosol formation (AP).

- Compare MOM chemistry to measurements obtained during the recent AQABA field campaign (HH).

- ~~Advancing~~ Advance our understanding of the role of organic compounds on the tropospheric O_x and HO_x budgets ~~.~~ (DT).

- Compare model results with studies at the SAPHIR chamber (DT).

- Investigate the multiphase chemical pathways leading to organic acids and aerosols ~~.~~ (DT).

- Simulate stratospheric isotope H exchanges between CH_4 and H_2O ~~.~~ (SG).

- ~~Implementation of~~ Implement additional photolysis modules (e.g., CLOUDJ, TUV) and ~~comparison of the resulting~~ *J* compare the resulting *j*-values ~~.~~ (HH).

- ~~Parallelization~~ Parallelize to distribute independent (e.g., Monte-Carlo or sensitivity) box model simulations on multiple cores ~~.~~ (HH).

- Study the impact of aromatic compounds on atmospheric chemistry (RS, manuscript in preparation).

Code and data availability

The CAABA/MECCA model code is available as a community model published under the GNU General Public License[4]. The model code can be found in the electronic supplement. In addition to the complete code, a list of chemical reactions, including rate coefficients and references (meccanism.pdf), and a User Manual (caaba_mecca_manual.pdf) are available in the manual/ directory of the supplement. For further information and updates, the MECCA web page at http://www.mecca.messy-interface.org can be consulted.

Author contributions

RS develops and maintains the CAABA/MECCA software. AB provided RADJIMT. DC provided the aromatic chemistry mechanism of MOM. FF added code to control the model output. JUG provided DISSOC and helped with its implementation in MESSy. SG provided the MECCA-TAG sub-submodel. HH and ST provided code for the inclusion of the MCM reaction schemes. PJ contributed to several model development projects (MESSy modeling system, PolyMECCA, CHEMPROP, CHEMGLUE) and maintains the interfaces to ensure that the modules are not only compatible with the box model but also with the 3D models. VH contributed through initiating the provision of CAMS chemistry models for inclusion in MECCA, and for generation of the CB05BASCOE merged chemical mechanism. VK integrated CB05BASCOE and MOZART into MECCA. KN provided code for the skeletal mechanism generation. AP contributed to several model development projects (MESSy modeling system, scenarios for skeletal mechanism generation, MOM, CAMS, PolyMECCA testing). HR provided an update of the TRAJECT submodel. MS provided JAM002, and DT provided MOM.

Supplementary material related to this article is available online at: https://doi.org/10.5194/gmd-0-1-2019-supplement.

Acknowledgements. We thank Simon Chabrillat and Idir Bouarar for provision of the mechanisms BASCOE and MOZART, respectively. We also thank Tim Butler for contributing the diagnostic tool check_eqns.pl. Duy Cai added some photolysis reactions to JVAL. Tilo Fytterer and Stefan Versick discovered and reported the temperature dependence bug of the ozone and OCS photolyses in JVAL. VH acknowledges funding from the Copernicus Atmosphere Monitoring Service (CAMS).

[4]http://www.gnu.org/copyleft/gpl.html

References

Arey, J., Aschmann, S. M., Kwok, E. S. C., and Atkinson, R.: Alkyl nitrate, hydroxyalkyl nitrate, and hydroxycarbonyl formation from the NO_x-air photooxidations of C_5-C_8 n-alkanes, J. Phys. Chem. A, 105, 1020–1027, doi:10.1021/jp003292z, 2001.

Assaf, E., Song, B., Tomas, A., Schoemaecker, C., and Fittschen, C.: Rate constant of the reaction between CH_3O_2 radicals and OH radicals revisited, J. Phys. Chem. A, 120, 8923–8932, doi:10.1021/acs.jpca.6b07704, 2016.

Assaf, E., Sheps, L., Whalley, L., Heard, D., Tomas, A., Schoemaecker, C., and Fittschen, C.: The reaction between CH_3O_2 radicals and OH radicals: Product yields and atmospheric implications, Environ. Sci. Technol., 51, 2170–2177, doi:10.1021/acs.est.6b06265, 2017.

Atkinson, R.: A structure-activity relationship for the estimation of rate constants for the gas-phase reactions of OH radicals with organic compounds, Int. J. Chem. Kinetics, 19, 799–828, doi:10.1002/kin.550190903, 1987.

Atkinson, R., Baulch, D. L., Cox, R. A., Crowley, J. N., Hampson, R. F., Hynes, R. G., Jenkin, M. E., Rossi, M. J., Troe, J., and IUPAC Subcommittee: Evaluated kinetic and photochemical data for atmospheric chemistry: Volume II – gas phase reactions of organic species, Atmos. Chem. Phys., 6, 3625–4055, doi:10.5194/ACP-6-3625-2006, 2006.

Barnes, I., Becker, K. H., and Zhu, T.: Near UV absorption-spectra and photolysis products of difunctional organic nitrates - possible importance as NO_x reservoirs, J. Atmos. Chem., 17, 353–373, doi:10.1007/BF00696854, 1993.

Baumgaertner, A. J. G., Jöckel, P., Aylward, A. D., and Harris, M. J.: Simulation of particle precipitation effects on the atmosphere with the MESSy model system, in: Climate and Weather of the Sun-Earth System (CAWSES). Highlights from a Priority Program, edited by Lübken, F.-J., pp. 301–316, Springer Verlag, Berlin, 2013.

Becker, G., Grooß, J.-U., McKenna, D. S., and Müller, R.: Stratospheric photolysis frequencies: Impact of an improved numerical solution of the radiative transfer equation, J. Atmos. Chem., 37, 217–229, doi:10.1023/A:1006468926530, 2000.

Bejan, I., Abd El Aal, Y., Barnes, I., Benter, T., Bohn, B., Wiesen, P., and Kleffmann, J.: The photolysis of ortho-nitrophenols: a new gas phase source of HONO, Phys. Chem. Chem. Phys., 8, 2028–2035, doi:10.1039/B516590C, 2006.

Birdsall, A. W., Andreoni, J. F., and Elrod, M. J.: Investigation of the role of bicyclic peroxy radicals in the oxidation mechanism of toluene, J. Phys. Chem. A, 114, 10 655–10 663, doi:10.1021/jp105467e, 2010.

Bloss, C., Wagner, V., Jenkin, M. E., Volkamer, R., Bloss, W. J., Lee, J. D., Heard, D. E., Wirtz, K., Martin-Reviejo, M., Rea, G., Wenger, J. C., and Pilling, M. J.: Development of a detailed chemical mechanism (MCMv3.1) for the atmospheric oxidation of aromatic hydrocarbons, Atmos. Chem. Phys., 5, 641–664, doi:10.5194/acp-5-641-2005, 2005.

Bossolasco, A., Faragó, E. P., Schoemaecker, C., and Fittschen, C.: Rate constant of the reaction between CH_3O_2 and OH radicals, Chem. Phys. Lett., 593, 7–13, doi:10.1016/j.cplett.2013.12.052, 2014.

Boyd, A. A., Flaud, P.-M., Daugey, N., and Lesclaux, R.: Rate constants for RO_2 + HO_2 reactions measured under a large excess of

HO_2, J. Phys. Chem. A, 107, 818–821, doi:10.1021/JP026581R, 2003.

Brasseur, G., Smith, A., Khosravi, R., Huang, T., Walters, S., Chabrillat, S., and Kockarts, G.: Natural and human-induced perturbations in the middle atmosphere: A short tutorial, in: Atmospheric Science Across the Stratopause, Geophysical Monograph 123, edited by Siskind, D. E., Eckermann, S. D., and Summers, M. E., pp. 7–20, Am. Geophys. Union, Washington, D.C., doi:10.1029/GM123p0007, 2000.

Brasseur, G. P. and Solomon, S.: Aeronomy of the Middle Atmosphere: Chemistry and Physics of the Stratosphere and Mesosphere, Springer Verlag, doi:10.1007/1-4020-3824-0, 2005.

Burkholder, J. B., Sander, S. P., Abbatt, J., Barker, J. R., Huie, R. E., Kolb, C. E., Kurylo, M. J., Orkin, V. L., Wilmouth, D. M., and Wine, P. H.: Chemical Kinetics and Photochemical Data for Use in Atmospheric Studies, Evaluation No. 18, JPL Publication 15-10, Jet Propulsion Laboratory, Pasadena, http://jpldataeval.jpl.nasa.gov, 2015.

Butkovskaya, N., Kukui, A., and Le Bras, G.: Pressure and temperature dependence of ethyl nitrate formation in the $C_2H_5O_2$ + NO reaction, J. Phys. Chem. A, 114, 956–964, doi:10.1021/jp910003a, 2010.

Butkovskaya, N., Kukui, A., and Le Bras, G.: Pressure and temperature dependence of methyl nitrate formation in the CH_3O_2 + NO reaction, J. Phys. Chem. A, 116, 5972–5980, doi:10.1021/jp210710d, 2012.

Cabrera-Perez, D., Taraborrelli, D., Sander, R., and Pozzer, A.: Global atmospheric budget of simple monocyclic aromatic compounds, Atmos. Chem. Phys., 16, 6931–6947, doi:10.5194/acp-16-6931-2016, 2016.

Capouet, M., Müller, J.-F., Ceulemans, K., Compernolle, S., Vereecken, L., and Peeters, J.: Modeling aerosol formation in alpha-pinene photo-oxidation experiments, J. Geophys. Res., 113D, doi:10.1029/2007JD008995, 2008.

Chabrillat, S. and Fonteyn, D.: Modelling long-term changes of mesospheric temperature and chemistry, Adv. Space Res., 32, 1689–1700, doi:10.1016/S0273-1177(03)90464-9, 2003.

Chen, J., Wenger, J. C., and Venables, D. S.: Near-ultraviolet absorption cross sections of nitrophenols and their potential influence on tropospheric oxidation capacity, J. Phys. Chem. A, 115, 12 235–12 242, doi:10.1021/jp206929r, 2011.

Cheng, S.-B., Zhou, C.-H., Yin, H.-M., Sun, J.-L., and Han, K.-L.: OH produced from *o*-nitrophenol photolysis: A combined experimental and theoretical investigation, J. Chem. Phys., 130, 234 311, doi:10.1063/1.3152635, 2009.

Clubb, A. E., Jordan, M. J. T., Kable, S. H., and Osborn, D. L.: Phototautomerization of acetaldehyde to vinyl alcohol: a primary process in UV-irradiated acetaldehyde from 295 to 335 nm, J. Phys. Chem. Lett., 3, 3522–3526, doi:10.1021/jz301701x, 2012.

Considine, D. B., Douglass, A. R., Connell, P. S., Kinnison, D. E., and Rotman, D. A.: A polar stratospheric cloud parameterization for the global modeling initiative three-dimensional model and its response to stratospheric aircraft, J. Geophys. Res., 105D, 3955–3973, doi:10.1029/1999JD900932, 2000.

Crounse, J. D., Knap, H. C., Ørnsø, K. B., Jørgensen, S., Paulot, F., Kjaergaard, H. G., and Wennberg, P. O.: Atmospheric fate of methacrolein. 1. peroxy radical isomerization following addition of OH and O_2, J. Phys. Chem. A, 116, 5756–5762, doi:10.1021/jp211560u, 2012.

da Silva, G.: Carboxylic acid catalyzed keto-enol tautomerizations in the gas phase, Angew. Chem., 122, 7685–7687, doi:10.1002/ange.201003530, 2010.

Dillon, T. J. and Crowley, J. N.: Direct detection of OH formation in the reactions of HO_2 with $CH_3C(O)O_2$ and other substituted peroxy radicals, Atmos. Chem. Phys., 8, 4877–4889, doi:10.5194/ACP-8-4877-2008, 2008.

Dobbin, A. L.: Modelling studies of possible coupling mechanisms between the upper and middle atmosphere, Ph.D. thesis, Department of Physics and Astronomy, University College London, http://discovery.ucl.ac.uk/1444625, 2005.

Dobbin, A. L. and Aylward, A. D.: A three-dimensional modelling study of the processes leading to mid latitude nitric oxide increases in the lower thermosphere following periods of high geomagnetic activity, Adv. Space Res., 42, 1576–1585, doi:10.1016/j.asr.2008.03.004, 2008.

Elrod, M. J.: Kinetics study of the aromatic bicyclic peroxy radical + NO reaction: overall rate constant and nitrate product yield measurements, J. Phys. Chem. A, 115, 8125–8130, doi:10.1021/jp204308f, 2011.

Emmons, L. K., Walters, S., Hess, P. G., Lamarque, J.-F., Pfister, G. G., Fillmore, D., Granier, C., Guenther, A., Kinnison, D., Laepple, T., Orlando, J., Tie, X., Tyndall, G., Wiedinmyer, C., Baughcum, S. L., and Kloster, S.: Description and evaluation of the Model for Ozone and Related chemical Tracers, version 4 (MOZART-4), Geosci. Model Dev., 3, 43–67, doi:10.5194/gmd-3-43-2010, 2010.

Errera, Q. and Fonteyn, D.: Four-dimensional variational chemical assimilation of CRISTA stratospheric measurements, J. Geophys. Res., 106D, 12 253–12 265, doi:10.1029/2001JD900010, 2001.

Errera, Q., Daerden, F., Chabrillat, S., Lambert, J. C., Lahoz, W. A., Viscardy, S., Bonjean, S., and Fonteyn, D.: 4D-Var assimilation of MIPAS chemical observations: ozone and nitrogen dioxide analyses, Atmos. Chem. Phys., 8, 6169–6187, doi:10.5194/acp-8-6169-2008, 2008.

Fennelly, J. A. and Torr, D. G.: Photoionization and photoabsorption cross sections of O, N_2, O_2, and N for aeronomic calculations, At. Data Nucl. Data Tables, 51, 321–363, doi:10.1016/0092-640X(92)90004-2, 1992.

Flocke, F., Atlas, E., Madronich, S., Schauffler, S. M., Aikin, K., Margitan, J. J., and Bui, T. P.: Observations of methyl nitrate in the lower stratosphere during STRAT: implications for its gas phase production mechanisms, Geophys. Res. Lett., 25, 1891–1894, doi:10.1029/98GL01417, 1998.

Frank, F., Jöckel, P., Gromov, S., and Dameris, M.: Investigating the yield of H_2O and H_2 from methane oxidation in the stratosphere, Atmos. Chem. Phys., 18, 9955–9973, doi:10.5194/acp-18-9955-2018, 2018.

Fuller-Rowell, T. J.: Modeling the solar cycle change in nitric oxide in the thermosphere and upper mesosphere, J. Geophys. Res., 98A, 1559–1570, doi:10.1029/92JA02201, 1993.

Glover, B. G. and Miller, T. A.: Near-IR cavity ringdown spectroscopy and kinetics of the isomers and conformers of the butyl peroxy radical, J. Phys. Chem. A, 109, 11 191–11 197, doi:10.1021/jp054838q, 2005.

Gromov, S., Jöckel, P., Sander, R., and Brenninkmeijer, C. A. M.: A kinetic chemistry tagging technique and its application to modelling the stable isotopic composition of atmospheric

trace gases, Geosci. Model Dev., 3, 337–364, doi:10.5194/GMD-3-337-2010, 2010.

Groß, C. B. M.: Kinetische Studien zur OH-Bildung über die Reaktionen von HO_2 mit organischen Peroxyradikalen, Ph.D. thesis, Johannes Gutenberg-Universität, 2013.

Groß, C. B. M., Dillon, T. J., Schuster, G., Lelieveld, J., and Crowley, J. N.: Direct kinetic study of OH and O_3 formation in the reaction of $CH_3C(O)O_2$ with HO_2, J. Phys. Chem. A, 1, 974–985, doi:10.1021/jp412380z, 2014.

Harris, M. J.: A new coupled middle atmosphere and thermosphere general circulation model: Studies of dynamic, energetic and photochemical coupling in the middle and upper atmosphere, Ph.D. thesis, Department of Physics and Astronomy, University College London, http://search.proquest.com/docview/1758611641, 2001.

Henke, B. L., Gullikson, E. M., and Davis, J. C.: X-Ray Interactions: Photoabsorption, Scattering, Transmission, and Reflection at E = 50-30,000 eV, Z = 1-92, At. Data Nucl. Data Tables, 54, 181–342, doi:10.1006/adnd.1993.1013, 1993.

Hens, K., Novelli, A., Martinez, M., Auld, J., Axinte, R., Bohn, B., Fischer, H., Keronen, P., Kubistin, D., Nölscher, A. C., Oswald, R., Paasonen, P., Petäjä, T., Regelin, E., Sander, R., Sinha, V., Sipilä, M., Taraborrelli, D., Tatum Ernest, C., Williams, J., Lelieveld, J., and Harder, H.: Observation and modelling of HO_x radicals in a boreal forest, Atmos. Chem. Phys., 14, 8723–8747, doi:10.5194/ACP-14-8723-2014, 2014.

Heue, K.-P., Riede, H., Walter, D., Brenninkmeijer, C. A. M., Wagner, T., ß, U. F., Platt, U., Zahn, A., Stratmann, G., and Ziereis, H.: CARIBIC DOAS observations of nitrous acid and formaldehyde in a large convective cloud, Atmos. Chem. Phys., 14, 6621–6642, doi:10.5194/acp-14-6621-2014, 2014.

Huijnen, V., Williams, J., van Weele, M., van Noije, T., Krol, M., Dentener, F., Segers, A., Houweling, S., Peters, W., de Laat, J., Boersma, F., Bergamaschi, P., van Velthoven, P., Le Sager, P., Eskes, H., Alkemade, F., Scheele, R., Nédélec, P., and Pätz, H.-W.: The global chemistry transport model TM5: description and evaluation of the tropospheric chemistry version 3.0, Geosci. Model Dev., 3, 445–473, doi:10.5194/gmd-3-445-2010, 2010.

Huijnen, V., Flemming, J., Chabrillat, S., Errera, Q., Christophe, Y., Blechschmidt, A.-M., Richter, A., and Eskes, H.: C-IFS-CB05-BASCOE: stratospheric chemistry in the Integrated Forecasting System of ECMWF, Geosci. Model Dev., 9, 3071–3091, doi:10.5194/gmd-9-3071-2016, 2016.

Huijnen, V., Pozzer, A., Arteta, J., Brasseur, G., Bouarar, I., Chabrillat, S., Christophe, Y., Doumbia, T., Flemming, J., Guth, J., Josse, B., Karydis, V. A., Marécal, V., and Pelletier, S.: Quantifying uncertainties due to chemistry modeling – evaluation of tropospheric composition simulations in the CAMS model, Geosci. Model Dev. Discuss., doi:10.5194/gmd-2018-331, 2019.

Jacobson, M. Z.: Fundamentals of atmospheric modeling, Cambridge University Press, Cambridge, 1999.

Jagiella, S. and Zabel, F.: Reaction of phenylperoxy radicals with NO_2 at 298 K, Phys. Chem. Chem. Phys., 9, 5036–5051, doi:10.1039/B705193J, 2007.

Jenkin, M., Saunders, S. M., and Pilling, M. J.: The tropospheric degradation of volatile organic compounds: A protocol for mechanism development, Atmos. Environ., 31, 81–104, doi:10.1016/S1352-2310(96)00105-7, 1997.

Jenkin, M. E., Shallcross, D. E., and Harvey, J. N.: Development and application of a possible mechanism for the generation of e^- cis-pinic acid from the ozonolysis of α- and β-pinene, Atmos. Environ., 34, 2837–2850, doi:10.1016/S1352-2310(00)00087-X, 2000.

Jenkin, M. E., Saunders, S. M., Wagner, V., and Pilling, M. J.: Protocol for the development of the Master Chemical Mechanism, MCM v3 (part B): tropospheric degradation of aromatic volatile organic compounds, Atmos. Chem. Phys., 3, 181–193, doi:10.5194/acp-3-181-2003, 2003.

Jenkin, M. E., Young, J. C., and Rickard, A. R.: The MCM v3.3.1 degradation scheme for isoprene, Atmos. Chem. Phys., 15, 11 433–11 459, doi:10.5194/acp-15-11433-2015, 2015.

Jöckel, P., Kerkweg, A., Buchholz-Dietsch, J., Tost, H., Sander, R., and Pozzer, A.: Technical Note: Coupling of chemical processes with the Modular Earth Submodel System (MESSy) submodel TRACER, Atmos. Chem. Phys., 8, 1677–1687, doi:10.5194/ACP-8-1677-2008, 2008.

Jöckel, P., Kerkweg, A., Pozzer, A., Sander, R., Tost, H., Riede, H., Baumgaertner, A., Gromov, S., and Kern, B.: Development cycle 2 of the Modular Earth Submodel System (MESSy2), Geosci. Model Dev., 3, 717–752, doi:10.5194/GMD-3-717-2010, 2010.

Jöckel, P., Tost, H., Pozzer, A., Kunze, M., Kirner, O., Brenninkmeijer, C. A. M., Brinkop, S., Cai, D. S., Dyroff, C., Eckstein, J., Frank, F., Garny, H., Gottschaldt, K.-D., Graf, P., Grewe, V., Kerkweg, A., Kern, B., Matthes, S., Mertens, M., Meul, S., Neumaier, M., Nützel, M., Oberländer-Hayn, S., Ruhnke, R., Runde, T., Sander, R., Scharffe, D., and Zahn, A.: Earth System Chemistry integrated Modelling (ESCiMo) with the Modular Earth Submodel System (MESSy, version 2.51), Geosci. Model Dev., 9, 1153–1200, doi:10.5194/gmd-9-1153-2016, 2016.

Kinnison, D. E., Brasseur, G. P., Walters, S., Garcia, R. R., Marsh, D. R., Sassi, F., Harvey, V. L., Randall, C. E., Emmons, L., Lamarque, J. F., Hess, P., Orlando, J. J., Tie, X. X., Randel, W., Pan, L. L., Gettelman, A., Granier, C., Diehl, T., Niemeier, U., and Simmons, A. J.: Sensitivity of chemical tracers to meteorological parameters in the MOZART-3 chemical transport model, J. Geophys. Res., 112D, doi:10.1029/2006JD007879, 2007.

Kirchner, F., Mayer-Figge, A., Zabel, F., and Becker, K. H.: Thermal stability of peroxynitrates, Int. J. Chem. Kinetics, 31, 127–144, doi:10.1002/(SICI)1097-4601(1999)31:2<127::AID-KIN6>3.0.CO;2-L, 1999.

Kwok, E. S. C. and Atkinson, R.: Estimation of hydroxyl radical reaction rate constants for gas-phase organic compounds using a structure-reactivity relationship: an update, Atmos. Environ., 29, 1685–1695, doi:10.1016/1352-2310(95)00069-B, 1995.

Lamarque, J.-F., Emmons, L. K., Hess, P. G., Kinnison, D. E., Tilmes, S., Vitt, F., Heald, C. L., Holland, E. A., Lauritzen, P. H., Neu, J., Orlando, J. J., Rasch, P. J., and Tyndall, G. K.: CAM-chem: description and evaluation of interactive atmospheric chemistry in the Community Earth System Model, Geosci. Model Dev., 5, 369–411, doi:10.5194/gmd-5-369-2012, 2012.

Landgraf, J. and Crutzen, P. J.: An efficient method for online calculations of photolysis and heating rates, J. Atmos. Sci., 55, 863–878, doi:10.1175/1520-0469(1998)055<0863:AEMFOC>2.0.CO;2, 1998.

Lary, D. J. and Pyle, J. A.: Diffuse radiation, twilight, and photochemistry — I, J. Atmos. Chem., 13, 373–406, doi:10.1007/BF00057753, 1991.

Lehmann, R.: An algorithm for the determination of all significant pathways in chemical reaction systems, J. Atmos. Chem., 47, 45–78, doi:10.1023/B:JOCH.0000012284.28801.B1, 2004.

Lelieveld, J., Gromov, S., Pozzer, A., and Taraborrelli, D.: Global tropospheric hydroxyl distribution, budget and reactivity, Atmos. Chem. Phys., 16, 12 477–12 493, doi:10.5194/acp-16-12477-2016, 2016.

Liu, Y. J., Herdlinger-Blatt, I., McKinney, K. A., and Martin, S. T.: Production of methyl vinyl ketone and methacrolein via the hydroperoxyl pathway of isoprene oxidation, Atmos. Chem. Phys., 13, 5715–5730, doi:10.5194/acp-13-5715-2013, 2013.

Madronich, S. and Calvert, J. G.: Permutation reactions of organic peroxy radicals in the troposphere, J. Geophys. Res., 95D, 5697–5715, doi:10.1029/JD095ID05P05697, 1990.

Mallik, C., Tomsche, L., Bourtsoukidis, E., Crowley, J. N., Derstroff, B., Fischer, H., Hafermann, S., Hüser, I., Javed, U., Keßel, S., Lelieveld, J., Martinez, M., Meusel, H., Novelli, A., Phillips, G. J., Pozzer, A., Reiffs, A., Sander, R., Taraborrelli, D., Sauvage, C., Schuladen, J., Su, H., Williams, J., and Harder, H.: Oxidation processes in the eastern Mediterranean atmosphere: evidence from the modelling of HO_x measurements over Cyprus, Atmos. Chem. Phys., 18, 10 825–10 847, doi:10.5194/acp-18-10825-2018, 2018.

McKenna, D. S., Grooß, J.-U., Günther, G., Konopka, P., Müller, R., Carver, G., and Sasano, Y.: A new chemical Lagrangian model of the stratosphere (CLaMS) 2. Formulation of chemistry scheme and initialization, J. Geophys. Res., 107D, doi:10.1029/2000JD000113, 2002.

Meier, R. R., Anderson, Jr., D. E., and Nicolet, M.: Radiation field in the troposphere and stratosphere from 240-1000 nm — I: General analysis, Planet. Space Sci., 30, 923–933, doi:10.1016/0032-0633(82)90134-9, 1982.

Messaadia, L., Dib, G. E., Ferhati, A., and Chakir, A.: UV-visible spectra and gas-phase rate coefficients for the reaction of 2,3-pentanedione and 2,4-pentanedione with OH radicals, Chem. Phys. Lett., 626, 73–79, doi:10.1016/j.cplett.2015.02.032, 2015.

Müller, J.-F., Peeters, J., and Stavrakou, T.: Fast photolysis of carbonyl nitrates from isoprene, Atmos. Chem. Phys., 14, 2497–2508, doi:10.5194/acp-14-2497-2014, 2014.

Müller, R., Peter, T., Crutzen, P. J., Oelhaf, H., Adrian, G. P., von Clarmann, T., Wegner, A., Schmidt, U., and Lary, D.: Chlorine chemistry and the potential for ozone depletion in the Arctic stratosphere in the winter of 1991/92, Geophys. Res. Lett., 21, 1427–1430, doi:10.1029/94GL00465, 1994.

Nakanishi, H., Morita, H., and Nagakura, S.: Electronic structures and spectra of the keto and enol forms of acetylacetone, Bull. Chem. Soc. Jpn., 50, 2255–2261, doi:10.1246/bcsj.50.2255, 1977.

Nguyen, T. L., Peeters, J., and Vereecken, L.: Theoretical study of the gas-phase ozonolysis of β-pinene ($C_{10}H_{16}$), Phys. Chem. Chem. Phys., 11, 5643–5656, doi:10.1039/b822984h, 2009.

Nicolet, M., Meier, R. R., and Anderson, Jr., D. E.: Radiation field in the troposphere and stratosphere from 240-1000 nm — II. Numerical analysis, Planet. Space Sci., 30, 935–983, doi:10.1016/0032-0633(82)90135-0, 1982.

Niemeyer, K. E. and Sung, C.-J.: On the importance of graph search algorithms for DRGEP-based mechanism reduction methods, Combust. Flame, 158, 1439–1443, doi:10.1016/j.combustflame.2010.12.010, 2011.

Niemeyer, K. E., Sung, C.-J., and Raju, M. P.: Skeletal mechanism generation for surrogate fuels using directed relation graph with error propagation and sensitivity analysis, Combust. Flame, 157, 1760–1770, doi:10.1016/j.combustflame.2009.12.022, 2010.

Nölscher, A., Butler, T., Auld, J., Veres, P., Muñoz, A., Taraborrelli, D., Vereecken, L., Lelieveld, J., and Williams, J.: Using total OH reactivity to assess isoprene photooxidation via measurement and model, Atmos. Environ., 89, 453–463, doi:10.1016/j.atmosenv.2014.02.024, 2014.

Orlando, J. J. and Tyndall, G. S.: Laboratory studies of organic peroxy radical chemistry: an overview with emphasis on recent issues of atmospheric significance, Chem. Soc. Rev., 41, 6294–6317, doi:10.1039/C2CS35166H, 2012.

Orlando, J. J., Tyndall, G. S., and Paulson, S. E.: Mechanism of the OH-initiated oxidation of methacrolein, Geophys. Res. Lett., 26, 2191–2194, doi:10.1029/1999GL900453, 1999.

Paulot, F., Crounse, J. D., Kjaergaard, H. G., Kürten, A., St. Clair, J. M., Seinfeld, J. H., and Wennberg, P. O.: Unexpected epoxide formation in the gas-phase photooxidation of isoprene, Science, 325, doi:10.1126/science.1172910, 2009.

Peeters, J., Boullart, W., Pultau, V., Vandenberk, S., and Vereecken, L.: Structure-activity relationship for the addition of OH to (poly)alkenes: Site-specific and total rate constants, J. Phys. Chem. A, 111, 1618–1631, doi:10.1021/jp066973o, 2007.

Peeters, J., Nguyen, T. L., and Vereecken, L.: HO_x radical regeneration in the oxidation of isoprene, Phys. Chem. Chem. Phys., 11, 5935–5939, doi:10.1039/B908511D, 2009.

Peeters, J., Müller, J.-F., Stavrakou, T., and Nguyen, V. S.: Hydroxyl radical recycling in isoprene oxidation driven by hydrogen bonding and hydrogen tunneling: the upgraded LIM1 mechanism, J. Phys. Chem. A, 118, 8625–8643, doi:10.1021/jp5033146, 2014.

Peixoto, T. P.: The graph-tool python library, Figshare, doi:10.6084/m9.figshare.1164194, 2014.

Pepiot-Desjardins, P. and Pitsch, H.: An efficient error-propagation-based reduction method for large chemical kinetic mechanisms, Combust. Flame, 154, 67–81, doi:10.1016/j.combustflame.2007.10.020, 2008.

Pommrich, R., Müller, R., Grooß, J.-U., Konopka, P., Ploeger, F., Vogel, B., Tao, M., Hoppe, C. M., Günther, G., Spelten, N., Hoffmann, L., Pumphrey, H.-C., Viciani, S., D'Amato, F., Volk, C. M., Hoor, P., Schlager, H., and Riese, M.: Tropical troposphere to stratosphere transport of carbon monoxide and long-lived trace species in the Chemical Lagrangian Model of the Stratosphere (CLaMS), Geosci. Model Dev., 7, 2895–2916, doi:10.5194/gmd-7-2895-2014, 2014.

Praske, E., Crounse, J. D., Bates, K. H., Kurtén, T., Kjaergaard, H. G., and Wennberg, P. O.: Atmospheric fate of methyl vinyl ketone: peroxy radical reactions with NO and HO_2, J. Phys. Chem. A, 119, 4562–4572, doi:10.1021/jp5107058, 2015.

Rickard, A. and Pascoe, S.: The Master Chemical Mechanism (MCM), http://mcm.leeds.ac.uk, 2009.

Riede, H., Jöckel, P., and Sander, R.: Quantifying atmospheric transport, chemistry, and mixing using a new trajectory-box model and a global atmospheric-chemistry GCM, Geosci. Model Dev., 2, 267–280, doi:10.5194/GMD-2-267-2009, 2009.

Sander, R., Kerkweg, A., Jöckel, P., and Lelieveld, J.: Technical note: The new comprehensive atmospheric chemistry module MECCA, Atmos. Chem. Phys., 5, 445–450, doi:10.5194/ACP-5-445-2005, 2005.

Sander, R., Baumgaertner, A., Gromov, S., Harder, H., Jöckel, P., Kerkweg, A., Kubistin, D., Regelin, E., Riede, H., Sandu, A., Taraborrelli, D., Tost, H., and Xie, Z.-Q.: The atmospheric chemistry box model CAABA/MECCA-3.0, Geosci. Model Dev., 4, 373–380, doi:10.5194/GMD-4-373-2011, 2011a.

Sander, R., Jöckel, P., Kirner, O., Kunert, A. T., Landgraf, J., and Pozzer, A.: The photolysis module JVAL-14, compatible with the MESSy standard, and the JVal PreProcessor (JVPP), Geosci. Model Dev., 7, 2653–2662, doi:10.5194/GMD-7-2653-2014, 2014.

Sander, S. P., Friedl, R. R., Golden, D. M., Kurylo, M. J., Moortgat, G. K., Keller-Rudek, H., Wine, P. H., Ravishankara, A. R., Kolb, C. E., Molina, M. J., Finlayson-Pitts, B. J., Huie, R. E., and Orkin, V. L.: Chemical Kinetics and Photochemical Data for Use in Atmospheric Studies, Evaluation Number 15, JPL Publication 06-2, Jet Propulsion Laboratory, Pasadena, CA, http://jpldataeval.jpl.nasa.gov, 2006.

Sander, S. P., Abbatt, J., Barker, J. R., Burkholder, J. B., Friedl, R. R., Golden, D. M., Huie, R. E., Kolb, C. E., Kurylo, M. J., Moortgat, G. K., Orkin, V. L., and Wine, P. H.: Chemical Kinetics and Photochemical Data for Use in Atmospheric Studies, Evaluation No. 17, JPL Publication 10-6, Jet Propulsion Laboratory, Pasadena, http://jpldataeval.jpl.nasa.gov, 2011b.

Sandu, A. and Sander, R.: Technical note: Simulating chemical systems in Fortran90 and Matlab with the Kinetic PreProcessor KPP-2.1, Atmos. Chem. Phys., 6, 187–195, doi:10.5194/ACP-6-187-2006, 2006.

Saunders, S. M., Jenkin, M. E., Derwent, R. G., and Pilling, M. J.: Protocol for the development of the Master Chemical Mechanism, MCM v3 (Part A): tropospheric degradation of non-aromatic volatile organic compounds, Atmos. Chem. Phys., 3, 161–180, doi:10.5194/ACP-3-161-2003, 2003.

Schultz, M. G., Stadtler, S., Schröder, S., Taraborrelli, D., Franco, B., Krefting, J., Henrot, A., Ferrachat, S., Lohmann, U., Neubauer, D., Siegenthaler-Le Drian, C., Wahl, S., Kokkola, H., Kühn, T., Rast, S., Schmidt, H., Stier, P., Kinnison, D., Tyndall, G. S., Orlando, J. J., and Wespes, C.: The chemistry climate model ECHAM6.3-HAM2.3-MOZ1.0, Geosci. Model Dev., 11, 1695–1723, doi:10.5194/gmd-11-1695-2018, 2018.

Sehested, J., Christensen, L. K., Nielsen, O. J., Bilde, M., Wallington, T. J., Schneider, W. F., Orlando, J. J., and Tyndall, G. S.: Atmospheric chemistry of acetone: Kinetic study of the $CH_3C(O)CH_2O_2 + NO/NO_2$ reactions and decomposition of $CH_3C(O)CH_2O_2NO_2$, Int. J. Chem. Kinetics, 30, 475–489, doi:10.1002/(SICI)1097-4601(1998)30:7<475::AID-KIN4>3.0.CO;2-P, 1998.

Smith, III, F. L. and Smith, C.: Numerical evaluation of Chapman's grazing incidence integral ch (X, χ), J. Geophys. Res., 77, 3592–3597, doi:10.1029/JA077i019p03592, 1972.

So, S., Wille, U., and da Silva, G.: Atmospheric chemistry of enols: a theoretical study of the vinyl alcohol + OH + O_2 reaction mechanism, Environ. Sci. Technol., 48, 6694–6701, doi:10.1021/es500319q, 2014.

Solomon, S. C., Hays, P. B., and Abreu, V. J.: The auroral 6300 Å emission - Observations and modeling, J. Geophys. Res., 93, 9867–9882, doi:10.1029/JA093iA09p09867, 1988.

Strickland, D. J. and Meier, R. R.: A photoelectron model for the rapid computation of atmospheric excitation rates, Tech. Rep. ADA122871, Naval Research Lab Washington DC, http://oai.dtic.mil/oai/oai?verb=getRecord&metadataPrefix=html&identifier=ADA122871, 1982.

Taraborrelli, D., Lawrence, M. G., Butler, T. M., Sander, R., and Lelieveld, J.: Mainz Isoprene Mechanism 2 (MIM2): an isoprene oxidation mechanism for regional and global atmospheric modelling, Atmos. Chem. Phys., 9, 2751–2777, doi:10.5194/ACP-9-2751-2009, 2009.

Taraborrelli, D., Lawrence, M. G., Crowley, J. N., Dillon, T. J., Gromov, S., Groß, C. B. M., Vereecken, L., and Lelieveld, J.: Hydroxyl radical buffered by isoprene oxidation over tropical forests, Nature Geosci., 5, 190–193, doi:10.1038/NGEO1405, 2012.

Teng, A. P., Crounse, J. D., Lee, L., St. Clair, J. M., Cohen, R. C., and Wennberg, P. O.: Hydroxy nitrate production in the OH-initiated oxidation of alkenes, Atmos. Chem. Phys., 15, 4297–4316, doi:10.5194/acp-15-4297-2015, 2015.

Tilmes, S., Lamarque, J.-F., Emmons, L. K., Kinnison, D. E., Marsh, D., Garcia, R. R., Smith, A. K., Neely, R. R., Conley, A., Vitt, F., Val Martin, M., Tanimoto, H., Simpson, I., Blake, D. R., and Blake, N.: Representation of the Community Earth System Model (CESM1) CAM4-chem within the Chemistry-Climate Model Initiative (CCMI), Geosci. Model Dev., 9, 1853–1890, doi:10.5194/gmd-9-1853-2016, 2016.

Tobiska, W. K., Woods, T., Eparvier, F., Viereck, R., Floyd, L., Bouwer, D., Rottman, G., and White, O. R.: The SOLAR2000 empirical solar irradiance model and forecast tool, J. Atmos. Sol.-Terr. Phys., 62, 1233–1250, doi:10.1016/S1364-6826(00)00070-5, 2000.

Tomlin, A. S. and Turányi, T.: Mechanism reduction to skeletal form and species lumping, in: Cleaner Combustion, edited by Battin-Leclerc, F., Simmie, J. M., and Blurock, E., pp. 447–466, Springer Verlag, Berlin, doi:10.1007/978-1-4471-5307-8_17, 2013.

Tyndall, G. S., Cox, R. A., Granier, C., Lesclaux, R., Moortgat, G. K., Pilling, M. J., Ravishankara, A. R., and Wallington, T. J.: The atmospheric chemistry of small organic peroxy radicals, J. Geophys. Res., 106D, 12 157–12 182, doi:10.1029/2000JD900746, 2001.

van Eijck, A., Opatz, T., Taraborrelli, D., Sander, R., and Hoffmann, T.: New tracer compounds for secondary organic aerosol formation from β-caryophyllene oxidation, Atmos. Environ., 80, 122–130, doi:10.1016/J.ATMOSENV.2013.07.060, 2013.

Vereecken, L. and Peeters, J.: H-atom abstraction by OH-radicals from (biogenic) (poly)alkenes: C–H bond strengths and abstraction rates, Chem. Phys. Lett., 333, 162–168, doi:10.1016/S0009-2614(00)01347-6, 2001.

Vereecken, L. and Peeters, J.: A theoretical study of the OH-initiated gas-phase oxidation mechanism of β-pinene ($C_{10}H_{16}$): first generation products, Phys. Chem. Chem. Phys., 14, 3802–3815, doi:10.1039/c2cp23711c, 2012.

Vereecken, L., Müller, J.-F., and Peeters, J.: Low-volatility poly-oxygenates in the OH-initiated atmospheric oxidation of α-pinene: impact of non-traditional peroxyl radical chemistry, Phys. Chem. Chem. Phys., 9, 5241–5248, doi:10.1039/b708023a, 2007.

Vereecken, L., Chakravarty, H. K., Bohn, B., and Lelieveld, J.: Theoretical study on the formation of H- and O-atoms, HONO, OH, NO, and NO_2 from the lowest lying singlet and triplet states

in ortho-nitrophenol photolysis, Int. J. Chem. Kinetics, 48, 785–795, doi:10.1002/kin.21033, 2016.

Wallington, T. J., Ammann, M., Cox, R. A., Crowley, J. N., Herrmann, H., Jenkin, M. E., McNeill, V., Mellouki, A., Rossi, M. J., and Troe, J.: IUPAC Task group on atmospheric chemical kinetic data evaluation: Evaluated kinetic data, http://iupac.pole-ether.fr, 2018.

Williams, J. E., van Velthoven, P. F. J., and Brenninkmeijer, C. A. M.: Quantifying the uncertainty in simulating global tropospheric composition due to the variability in global emission estimates of Biogenic Volatile Organic Compounds, Atmos. Chem. Phys., 13, 2857–2891, doi:10.5194/acp-13-2857-2013, 2013.

Wolfe, G. M., Crounse, J. D., Parrish, J. D., Clair, J. M. S., Beaver, M. R., Paulot, F., Yoon, T. P., Wennberg, P. O., and Keutsch, F. N.: Photolysis, OH reactivity and ozone reactivity of a proxy for isoprene-derived hydroperoxyenals (HPALDs), Phys. Chem. Chem. Phys., 14, 7276–7286, doi:10.1039/c2cp40388a, 2012.

Xiang, B., Zhu, L., and Tang, Y.: Photolysis of 4-oxo-2-pentenal in the 190-460 nm region, J. Phys. Chem. A, 111, 9025–9033, doi:10.1021/jp0739972, 2007.

Yarwood, G., Rao, S., Yocke, M., and Whitten, G.: Updates to the carbon bond chemical mechanism: CB05, Final report RT-04-00675, United States Environmental Protection Agency, http://www.camx.com/files/cb05_final_report_120805.aspx, 2005.